JOURNAL OF COMPUTATIONAL PHYSICS **147,** 187–218 (1998)
ARTICLE NO. CP986088

Effective Boundary Conditions for Laminar Flows over Periodic Rough Boundaries

Yves Achdou,* O. Pironneau,†,[1] and F. Valentin‡

**INSA Rennes, 20 Av des Buttes de Coesmes, 35043 Rennes, France; †Université Paris 6, 75252 Paris cedex 05; ‡INRIA Rocquencourt, 78153 Le Chesnay Cedex France*
E-mail: pironneau@an.jussieu.fr, frederic.valentin@inria.fr

Received December 18, 1997; revised June 25, 1998

Effective boundary conditions or wall laws are proposed for a laminar flow over a rough wall with periodic roughness elements. These effective conditions are posed on a regularized boundary which allows the details of the wall to be avoided and dramatically reduces the computational cost. The effective conditions stem from an asymptotic expansion of the solution, which is presented here. Both first- and second-order conditions are discussed and tested numerically on bidimensional cases.

1. INTRODUCTION

Rough boundaries are a challenge to numerical simulations because they are difficult to discretize and they require many mesh nodes near them even with unstructured meshes.

Yet there are many practical problems which have rough boundaries; electromagnetic scattering by an obstacle coated with an absorbing inhomogeneous paint and flow over rough surfaces are two such instances. Space shuttles covered with tiles for heat control are in this class because the tiles cannot be joined together exactly to account for dilatation and so the shuttle wall has an array of periodic gaps between the tiles.

This problem was studied mathematically for the Maxwell equations in [1, 4]. For flow problems, Carreau *et al*. have proposed a method in [6, 7] (analyzed later in [2, 3]) which is strikingly simple.

Consider for simplicity an incompressible viscous fluid. Assume that at some distance above the rough wall Γ^ε (where ε stands for the characteristic dimensions of the roughness elements) the flow is smooth. Then, for computational purposes, choose in that smooth region an artificial smooth boundary Γ^η above Γ^ε, parallel to the rough wall. If we knew the velocity v of the flow on Γ^η then the region below Γ^η could be forgotten in the computation

[1] This research was partially supported by Conselho Nacional de Pesquisa (CNPq), Brazil.

0021-9991/98 $25.00

and the problem would not have this small scale ε anymore. In addition, since v is known on Γ^η a computation of the flow below Γ^η could also be done and the normal stress component $\sigma \cdot n$ could be computed; obviously

$$\sigma \cdot n = F(v). \tag{1}$$

But since the domain between Γ^ε and Γ^η is thin, it is reasonable to think that F is a local function of v (i.e., $\sigma \cdot n(x) = F(v(x))$). So F could be tabulated beforehand as a function of the roughness geometry and Eq. (1) would be used as a new *effective* boundary condition on Γ^η.

Such effective conditions are known in the engineering community [15] and most often they are established in an empirical manner [11, 8].

At this point, two questions arise

1. Can the function F be constructed analytically, instead of being found empirically?
2. How precise is such an approach?

In this paper, we wish to answer these questions for laminar flows over periodic rough walls.

First let us note that this change of boundary conditions can be done even for smooth boundaries by a simple Taylor expansion. Indeed if $\eta(x)$ is the distance from Γ^η to the wall in the normal direction n, then

$$u(x + \eta(x)n(x)) = u(x) + \eta(x)\frac{\partial u}{\partial n}(x) + o(\eta) \quad \forall x \in \Gamma^\eta. \tag{2}$$

So the no-slip condition on the actual wall can be replaced by the condition on Γ^η,

$$u(x) + \eta(x)\frac{\partial u}{\partial n}(x) = 0 \quad \forall x \in \Gamma^\eta, \tag{3}$$

and obviously the method is of order one in η.

Of course this argument does not work when Γ^ε is rough. However, we will show that the result is still valid when the wall is periodic, provided that in (3) η is replaced by another scalar α, computed by solving a local Stokes problem in a cell containing one of the roughness elements of Γ^ε. This means in practice that Γ^ε is seen by the far field flow like a smooth wall at an effective distance of α.

In turbulence [14] a similar idea is used with wall laws. The velocity at a distance y from the wall is approximately

$$u(y) = u^*\left[\chi^{-1}\log\left(\frac{yu^*}{\nu}\right) + \beta\right], \quad \text{where } u^* = \sqrt{\nu\partial_y u}|_{y=0} \tag{4}$$

and where $\chi = 0.41$ is the Von Karman constant and β is a numerical constant which depends on the roughness of the wall. In view of the Taylor expansion (3), β is the effective height of the wall due to its roughness.

In electromagnetics such boundary conditions were introduced long ago by Leontovitch and, because the Maxwell equations are linear, the analysis can be carried out by a multiple scales expansion as in [1, 4]. Similar ideas can also be found in Keller [13]. The result is that conditions like (1) are first order in ε but that they can be generalized to more complex ones

that are accurate to any order. The domain decomposition argument of (1) was analyzed in [2]. Comprehensive surveys of multiple scale expansions can be found in Bensoussan *et al*. [5] and Sanchez-Palencia [17].

To extend the analysis to the Navier–Stokes equation one is faced with the problem of boundary layers. Will roughness be well within the boundary layer?; will it induce transition to turbulence or separation? We feel that for laminar flow the answer to these questions depends on the size of the Reynolds number Re, compared to the characteristic length of the roughness ε. First, we observe that for laminar flows the roughness elements are contained in the Prandtl boundary layer if

$$\frac{\varepsilon}{L} \ll \mathrm{Re}^{-1/2}.$$

If this is not the case, the boundary layer will be small, compared with the roughness, and the flow is likely to separate, at least locally. Thus, the full Navier–Stokes equations need to be considered, and the geometry cannot be simplified.

Now if the roughness elements lie within the boundary layer, the local Reynolds number in the roughness elements is

$$\frac{v\varepsilon}{\nu} \approx \frac{\partial v}{\partial n}\frac{\varepsilon^2}{\nu} \approx \frac{\varepsilon^2}{L^2}\mathrm{Re}^{3/2}.$$

Therefore, if $\varepsilon/L \ll \mathrm{Re}^{-3/4}$, then the viscous effects dominate in the roughness elements and the flow near the rough wall will tend to be Stokes-like, with corrections due to convection. If, on the contrary, $\mathrm{Re}^{-1/2} \gg \varepsilon/L \gg \mathrm{Re}^{-3/4}$, then the convection effects dominate. In this analysis, we consider periodic roughness and the special regime $\varepsilon\mathrm{Re}/L = O(1)$ which belongs to the first case above, and we will include in the asymptotic expansion both the diffusive and the convective effects. The numerical experiments confirm that it is meaningful for applications.

To readers who are not familiar with homogenization (multiple scale asymptotics), considering periodic roughness may seem restricted, but this is sort of usual in this field. Composite materials are not always periodic and yet the analysis of the periodic case gives a lot of information [5, 17]. Also, all the asymptotic regimes should be studied and, in particular, the cases $\varepsilon/L \gg \mathrm{Re}^{-3/4}$; but they seem to pose some mathematical and computational problems that we hope to solve in the future.

It would not be hard to extend the results to the Reynolds-averaged Navier–Stokes equation closed by a k-epsilon model, for instance, but the problem is: what is a good turbulence model near a rough wall? One major application would be for the modeling of turbulent flow over water waves. Perhaps the next step in this line would be rather to consider time-dependent flows. Then again, similar effective conditions would hold if the time variations are large, compared with the time scale derived from the roughness, which is often the case. Otherwise the problem seems more difficult. A time periodic flow can be analyzed, but that, too, is not turbulence.

This paper, therefore, is not the complete story for flows over rough walls; it can handle laminar flow at high Reynolds number ($O(\varepsilon^{-1})$) but not turbulent flow. It is a rigorous analysis within the usual limits for incompressible viscous Newtonian flow, namely that the solution of the Navier–Stokes equations exists, is locally unique, and is smooth. It validates first- and second-order conditions on smooth mean boundaries which are therefore useful numerically because the details of the boundary need not be taken into account.

The outline of the paper is the following: Section 2 contains a description of the problem. The first-order effective condition is obtained in Section 3; it is shown that it is equivalent to a mean flat wall between the min and max height of the roughness. Then the second-order effective boundary condition is derived and discussed in Section 4. These conditions should be used for additional precision or in certain cases when the roughness type changes at places as illustrated in the numerical section. Second-order conditions are no longer equivalent to a wall displacement and, interestingly enough, they are nonlinear. Numerical tests for two types of geometries are presented in Section 5. The first- and second-order conditions are compared to simulations with a full treatment of the smallest geometrical length scale. Good precision is obtained and validates the theory.

2. DESCRIPTION OF THE PROBLEM

2.1. *Description of the Geometry*

In the following, we give a description of a domain Ω^ε of the plan $\mathbb{R}^2$ whose boundary is partly rough with periodic roughness elements. Although the situation is rather clear on Fig. 1 and Fig. 2, a mathematical description is needed for the coming development.

Let (e_1, e_2) be an orthonormal basis of the plan $\mathbb{R}^2$ and let Y be a domain of $\mathbb{R}^2$, semi-infinite in the e_2 direction, such that the boundary of Y is decomposed into four parts (see Fig. 1),

$$\partial Y = \partial Y_1 \cup \partial Y_2 \cup \partial Y_3 \cup \partial Y_4,$$

with

$$\partial Y_1 = \{0\} \times [0, \infty[,$$
$$\partial Y_2 = \{2\pi\} \times [0, \infty[,$$

and ∂Y_3 is a bounded curve made of one piece such that

$$\partial Y_1 \cap \partial Y_3 = \{(0, 0)\},$$
$$\partial Y_2 \cap \partial Y_3 = \{(2\pi, 0)\}.$$

Finally, ∂Y_4 is the boundary of a finite number of obstacles (possibly empty) strictly contained in the domain delimited by $\partial Y_1 \cup \partial Y_2 \cup \partial Y_3$. We also assume that Y is contained in the half plane $x_2 > 0$. Thus zero is the infimum of the coordinate x_2 of a point in Y.

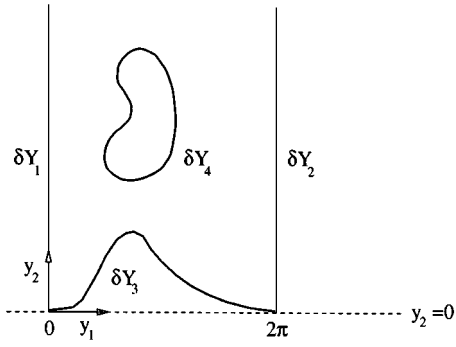

FIG. 1. The cell Y.

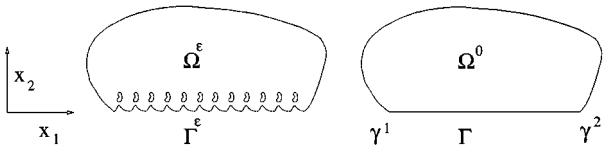

FIG. 2. The domains Ω^ε and Ω^0.

Let ε be a small positive real number, and let Y^ε be the image of Y by the dilatation of ratio ε and center $(0, 0)$. Let Θ^ε be the semi-infinite domain of $\mathbb{R}^2$ obtained by merging together all the images of Y^ε by the translations by $2\pi k\varepsilon e_1$, where k takes all the integer values. The infinite domain Θ^ε is contained in the half plane $x_2 > 0$.

Let Ω be a bounded domain of $\mathbb{R}^2$ intersecting the line $\{x_2 = 0\}$. We denote by Ω° the domain $\Omega \cap \{x_2 > 0\}$ (for simplicity, we suppose that Ω^0 is made of one piece), and we set $\Gamma = \partial\Omega^\circ \cap \{x_2 = 0\} = (\gamma_1, \gamma_2) \times \{0\}$.

Consider now $\Theta^\varepsilon \cap \Omega$. This set is nonempty, since Θ^ε touches the line $\{x_2 = 0\}$. For ε small enough, $\Theta^\varepsilon \cap \Omega$ has a fast oscillating rough boundary with wavelength $2\pi\varepsilon$. The amplitude of the roughness is also of order ε. We note $\Omega^\varepsilon = \Theta^\varepsilon \cap \Omega$ and Γ^ε is the rough part of $\partial\Omega^\varepsilon$. When $\varepsilon \to 0$, $\overline{\Omega^\varepsilon}$ converges to $\overline{\Omega^\circ}$ (see Fig. 2).

In the following, we shall use the notation (x_1, x_2) for the macroscopic variables and (y_1, y_2) for the microscopic variables:

$$y_i = x_i/\varepsilon.$$

Remark 2.1. For simplicity, we have chosen to work in two dimensions. Of course, all that follows can be generalized to the three-dimensional case.

2.2. *The Main Assumptions*

The basic problem consists of predicting the drag and the friction generated by a viscous fluid over the rough surface Γ^ε.

We consider a flow modeled by the usual steady-state incompressible Navier–Stokes equations,

$$\begin{aligned} u^\varepsilon \cdot \nabla u^\varepsilon - \nu\Delta u^\varepsilon + \nabla p^\varepsilon &= f \quad \text{in } \Omega^\varepsilon, \\ \nabla \cdot u^\varepsilon &= 0 \quad \text{in } \Omega^\varepsilon, \\ u^\varepsilon &= 0 \quad \text{on } \partial\Omega^\varepsilon. \end{aligned}$$

For simplicity, we assume that the support of the source term f does not intersect Γ^ε.

Remark 2.2. Of course, it is possible to propose more complex boundary conditions. For example, if the boundary $\partial\Omega^\varepsilon$ is partitioned into two parts: $\partial\Omega^\varepsilon = \partial\Omega_1 \cup \partial\Omega_2^\varepsilon$, with $\Gamma^\varepsilon \subset \partial\Omega_2^\varepsilon$, a possible set of boundary conditions is

$$\begin{aligned} u^\varepsilon &= u_1 \quad \text{on } \partial\Omega_1, \\ u^\varepsilon &= 0 \quad \text{on } \partial\Omega_2^\varepsilon. \end{aligned}$$

The coefficient ν is the viscosity. When ν is small, the flow exhibits boundary layers near the walls. Thus, the problem has three characteristic lengths: in addition to the macroscopic

scale (linked to Ω and f) of order $O(1)$, there are the Prandtl boundary layer scale (of order $\sqrt{\nu}$ for laminar flows) and the roughness scale ε. We are interested in the case when these scales are well separated and, especially, when

$$\sqrt{\nu} \gg \varepsilon.$$

In this case, it is reasonable to expect a viscous sublayer of size $O(\varepsilon)$ due to the roughness elements inside the Prandtl boundary layer.

For simplicity we shall focus on the asymptotical regime

$$\nu = \mu\varepsilon.$$

Therefore, the problem of interest for us is

$$\begin{aligned} u^\varepsilon \cdot \nabla u^\varepsilon - \mu\varepsilon \Delta u^\varepsilon + \nabla p^\varepsilon &= f \quad \text{in } \Omega^\varepsilon, \\ \nabla \cdot u^\varepsilon &= 0 \quad \text{in } \Omega^\varepsilon, \\ u^\varepsilon &= 0 \quad \text{on } \partial\Omega^\varepsilon. \end{aligned} \tag{5}$$

Of course, other regimes are possible and lead to other asymptotic expansions, but one has to keep in mind that asymptotic expansions are rather artificial since for realistic cases; the viscosity and the geometry are both given and fixed.

We shall also assume enough regularity on the data such that all the Navier–Stokes problems that we shall introduce below have isolated branches of solutions, corresponding to laminar regimes. This is, however, mathematically an open problem since the domain Ω^ε also depends on ε.

In the coming development, we shall call $\mathcal{L}^\varepsilon$ the partial differential operator

$$\mathcal{L}^\varepsilon(u, p) = u \cdot \nabla u - \mu\varepsilon \Delta u + \nabla p. \tag{6}$$

In what follows, we shall make the important assumption that the mean flow is not too much affected by the roughness; i.e., the solution of (5) is a perturbation of the solution of the problem:

$$\begin{aligned} u^\circ \cdot \nabla u^\circ - \mu\varepsilon \Delta u^\circ + \nabla p^\circ &= f \quad \text{in } \Omega^\circ, \\ \nabla \cdot u^\circ &= 0 \quad \text{in } \Omega^\circ, \\ u^\circ &= 0 \quad \text{on } \partial\Omega^\circ. \end{aligned} \tag{7}$$

In the case of the linear Stokes equations or other linear equations [1, 2, 4], this assumption can in fact be rigorously proven. The solution (u°, p°) of (7) will be referred to as the zeroth-order approximation of $(u^\varepsilon, p^\varepsilon)$. This approximation just consists of approaching the rough wall by Γ $(x_2 = 0)$.

We also assume that the solution of the above system describes a laminar flow; i.e., the Prandtl length scales apply on Γ,

$$\frac{\partial u^\circ}{\partial x_2} = O(\nu^{-1/2}), \quad \frac{\partial^2 u^\circ}{\partial x_2^2} = O(\nu^{-1}), \quad \frac{\partial^2 u^\circ}{\partial x_1 \partial x_2} = O(\nu^{-1/2}). \tag{8}$$

For a turbulent regime, the same work as below can be carried out, at least when the roughness remains in the viscous sublayer. This will done in a forthcoming work.

3. THE FIRST-ORDER ASYMPTOTIC EXPANSION AND THE RELATED EFFECTIVE CONDITION

We first discuss the implementation of the first-order effective boundary condition, namely what has to be done in practice. The algorithm below is the practical result of the ansatz given in Section 3.3. Therefore, Section 3.1 can be seen as a summary of the main results, whose justifications are given in Sections 3.3 and 6.

3.1. *The First-Order Effective Boundary Conditions; The Practical Implementation*

For practical reasons, the effective boundary condition will not be imposed on Γ, but slightly above; for that, let δ be a positive real number. We introduce Ω^δ the subset of Ω° given by

$$\Omega^\delta = \Omega^\circ \cap \{x_2 > \delta\varepsilon\}, \tag{9}$$

and we denote by Γ^δ,

$$G^\delta = \partial\Omega^\delta \cap \{x_2 = \delta\varepsilon\}. \tag{10}$$

See Fig. 3 (we will choose δ later). We propose to approximate $(u^\varepsilon, p^\varepsilon)$ in Ω^δ by (u^1, p^1), the solution of the effective boundary value problem,

$$\begin{aligned} u^1 \cdot \nabla u^1 - \mu\varepsilon\Delta u^1 + \nabla p^1 &= f \quad \text{in } \Omega^\delta, \\ \nabla \cdot u^1 &= 0 \quad \text{in } \Omega^\delta, \\ u^1 &= 0 \quad \text{on } \partial\Omega^\delta \backslash \Gamma^\delta, \\ \varepsilon\mu \frac{\partial u_1^1}{\partial n} + \frac{\mu}{\overline{\chi^1} + \delta} u_1^1 &= 0 \quad \text{on } \Gamma^\delta \\ u_2^1 &= 0 \quad \text{on } \Gamma^\delta, \end{aligned} \tag{11}$$

where u_1^1, u_2^1 are the two components of u^1.

Here the constant $\overline{\chi^1}$ is found by solving the *cell problem* in the cell Y; find the velocity field χ^1 and the pressure field π^1 defined in Y, and the constant parameter $\overline{\chi^1}$ such that

- χ^1 and π^1 are 2π-periodic in the horizontal variable (noted y_1).

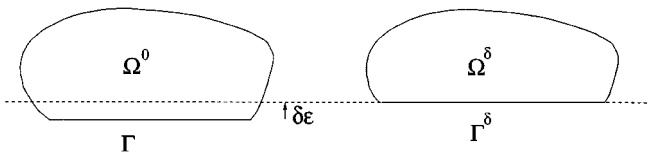

FIG. 3. The domain Ω^δ.

• $\chi^1 - \overline{\chi^1} e_1, \pi^1$ and all their derivatives decay fast (exponentially, in fact) as the vertical variable (noted y_2) grows.
•

$$\begin{aligned} -\mu\Delta\chi^1 + \nabla\pi^1 &= 0 && \text{in } Y, \\ \nabla\cdot\chi^1 &= 0 && \text{in } Y, \\ \chi^1 &= -y_2\, e_1 && \text{on } \partial Y_3 \cup \partial Y_4. \end{aligned} \tag{12}$$

It will be proved that this problem has a unique solution (see Section 6.1).

It can also be proved (cf. Theorem 3.2 below) that the constant $-\varepsilon\overline{\chi^1}$ is positive and smaller than the amplitude of the roughness elements. Therefore, if δ is chosen such that $\delta\varepsilon$ is greater than the amplitude of the roughness elements, the Navier-Stokes problem (11) is well posed because $\overline{\chi^1} + \delta > 0$.

To summarize, in order to compute the approximation (u^1, p^1) of $(u^\varepsilon, p^\varepsilon)$, it is necessary to:

1. approximate numerically the solution of the cell problem in $(\chi^1, \pi^1, \overline{\chi^1})$, by a finite element method, for example.
2. solve the Navier–Stokes problem (11) in the domain Ω^δ.

Let us emphasize that these results above apply to periodic roughness, as will be clear from the asymptotic expansion below. They may be generalized to perturbations of periodic geometries, for example when the wall Γ^ε is parametrized by the product of a smooth function of x_1 times a periodic function of x_1/ε.

To our knowledge, such a constructive approach is not known for (random) general roughness.

Note also that the constant $\overline{\chi^1}$ depends only on the geometry and not on the average flow; thus, its computation is completely independent. Computing the constant $\overline{\chi^1}$ is not very time-consuming, since only one period is considered, and the grid need not be very fine (there are no fast scales in the cell problem (12)). Then, the numerical approximation of (u^1, p^1) is much cheaper than that of $(u^\varepsilon, p^\varepsilon)$, simply because the geometry is simpler and the mesh does not need to be refined much in the horizontal direction. This will be well illustrated by the numerical tests below.

For nonstationary problems, there can be a fast time scale related to the roughness. However, it is sensible to think that in the rough region, the flow relaxes quickly in the fast time variable so the the mean flow does not have fast variations in time. In this case, we would look for boundary layers that are corrector independent of the fast time variable (steady state in the fast time variable). The same ansatz as below would show that the cell problem would be exactly (12), because the time derivative does not appear at leading order. Therefore, only the steady state solution of the cell problem is of interest, and exactly the same procedure as for stationary problems can be used. The cell problems must be solved once and for all, before starting the time scheme, so the computation of $\overline{\chi^1}$ is not expensive.

Note, finally, that this method does not work if the flow far away from the roughness has fast time or space scales, compared to those induced by the roughness.

3.2. *Preliminary on the Two Scales Expansion*

Before starting the description of the ansatz, we introduce the rules of calculus which will be used in the multiple scales expansion below; in the following, we will consider

functions $\Phi(x, y), x \in \Omega^\circ, y \in Y, 2\pi$-periodic in the variable y_1. We will associate to Φ the function $\Phi(x, x/\varepsilon)$. We introduce the operators of derivation with respect to the fast variable: the partial derivative with respect to y_i is denoted $\partial/\partial y_i$; $\nabla_y = (\partial/\partial y_1, \partial/\partial y_2)$ is the gradient with respect to y. In the same manner one can define the Laplace and the divergence operators Δ_y, ∇_y.

In order to present the computations in a simple form it is useful to consider first x and y as independent variables and to replace next y by x/ε. The rule of derivation is the following: applied to $\Phi(x, x/\varepsilon)$, the operator $\partial/\partial x_i$ becomes

$$\frac{\partial}{\partial x_i} + \frac{1}{\varepsilon}\frac{\partial}{\partial y_i}.$$

Note that this rule of computation is rigorous when dealing with products $\Phi = f(x)g(x/\varepsilon)$ and is formal in the general case. However, these rules can be justified mathematically.

3.3. *The Ansatz*

Here, we show how the results summarized in Section 3.1 are obtained. In order to improve the approximation of u^ε and p^ε, we propose the following ansatz:

$$\begin{aligned} u^\varepsilon(x) &\approx u^1(x) + \varepsilon u^1_{BL}\left(x, \frac{x}{\varepsilon}\right), \\ p^\varepsilon(x) &\approx p^1(x) + \varepsilon p^1_{BL}\left(x, \frac{x}{\varepsilon}\right). \end{aligned} \tag{13}$$

Here $u^1_{BL}(x, x/\varepsilon)$ and $p^1_{BL}(x, x/\varepsilon)$ decay exponentially fast as the variable x_2/ε tends to infinity and they are essentially periodic in the variable x_1/ε. Therefore, $u^1_{BL}(x, x/\varepsilon)$ and $p^1_{BL}(x, x/\varepsilon)$ are called *boundary layer correctors*. The terms $u^1(x)$ and $p^1(x)$ are called the *macroscopic first-order corrections* of u° and p° because they do not depend on the fast variable x/ε.

Remark 3.1. As it will appear from (15) below, when (8) is satisfied, $\varepsilon u^1_{BL}(x, x/\varepsilon)$ and $\varepsilon p^1_{BL}(x, x/\varepsilon)$ are of order $\sqrt{\varepsilon}$ for $x/\varepsilon \approx 0$. The small parameter in the asymptotic expansion is $\sqrt{\varepsilon}$, not ε.

More precisely, these functions are obtained by carrying out the following steps:

Step 1. We evaluate the error made by replacing $(u^\varepsilon, p^\varepsilon)$ by (u°, p°) in (5). In fact the error comes from the fact that the no-slip conditions on the rough wall Γ^ε are not satisfied by u°. However, since u° vanishes on Γ and since Γ^ε is close to Γ, the error should be small and is given by a Taylor expansion in the x_2 variable: $\forall x \in \Gamma^\varepsilon$

$$u^\circ(x) = \varepsilon \frac{\partial u^\circ}{\partial x_2}(x_1, 0)\frac{x_2}{\varepsilon} + \varepsilon^2 \frac{\partial^2 u^\circ}{\partial x_2^2}(x_1, 0)\left(\xi(x)\frac{x_2}{\varepsilon}\right)^2, \quad 0 < \xi < 1.$$

Here, the assumption that (7) describes a laminar flow implies that, at leading order,

$$u^\circ(x) \approx \varepsilon \frac{\partial u^\circ}{\partial x_2}(x_1, 0)\frac{x_2}{\varepsilon} \quad \text{on } \Gamma^\varepsilon. \tag{14}$$

Furthermore, from the no-slip boundary condition on Γ and since u° is divergence free,

$$\frac{\partial u^\circ}{\partial x_2}(x_1, 0) = \frac{\partial u_1^\circ}{\partial x_2}(x_1, 0)\, e_1,$$

where u_1° is the first component of u°.

Step 2. We see that the error in (14) at leading order is the product of a function of the macroscopic variable x_1, namely $\varepsilon(\partial u_1^\circ/\partial x_2)(x_1, 0)$ times a fast oscillating periodic term in the variable x_1, namely x_2/ε on Γ^ε, seen as a function (possibly multivalued) of x_1. Therefore, it is natural to look for $u_{BL}^1(x, x/\varepsilon)$ and $p_{BL}^1(x, x/\varepsilon)$ as the products of $(\partial u_1^\circ/\partial x_2)(x_1, 0)$ times functions of the fast variable x/ε, periodic in the horizontal direction and fast decaying in the vertical direction. Let us look for $u_{BL}^1(x, x/\varepsilon)$ and $p_{BL}^1(x, x/\varepsilon)$ of the form

$$\begin{aligned} u_{BL}^1\left(x, \frac{x}{\varepsilon}\right) &= \frac{\partial u_1^\circ}{\partial x_2}(x_1, 0)\left(\chi^1\left(\frac{x}{\varepsilon}\right) - \langle \chi^1 \rangle\right) \\ p_{BL}^1\left(x, \frac{x}{\varepsilon}\right) &= \frac{\partial u_1^\circ}{\partial x_2}(x_1, 0)\pi^1\left(\frac{x}{\varepsilon}\right), \end{aligned} \tag{15}$$

where $\langle \chi^1 \rangle$ is a constant vector, $\chi^1(x/\varepsilon)$ and $\pi^1(x/\varepsilon)$ are 2π-periodic functions in the variable x_1/ε, such that $\chi^1(x/\varepsilon) - \langle \chi^1 \rangle$ and π^1 decay fast as x_2/ε grows. The reason for writing the constant vector $\langle \chi^1 \rangle$ separately will appear soon. In the following we shall denote by $\mathcal{S}_{\text{per}}(Y)$ the space of the functions in Y, fast decaying in the variable y_2 as well as all their derivatives, 2π-periodic in the variable y_1.

Step 3. Let us plug $u^\circ + \varepsilon u_{BL}^1(x, x/\varepsilon)$ and $p^\circ + \varepsilon p_{BL}^1(x, x/\varepsilon)$ in (5):

$$\begin{aligned} \mathcal{L}^\varepsilon\left(u^\circ + \varepsilon u_{BL}^1,\, p^\circ + \varepsilon p_{BL}^1\right) - f\big) = \frac{\partial u_1^\circ}{\partial x_2}(x_1, 0)\big(-\mu \Delta_y \chi^1 + \nabla_y \pi^1\big) \\ + \text{smaller order terms.} \end{aligned} \tag{16}$$

The convective term $(\partial u_1^\circ/\partial x_2)(x_1, 0)u^\circ \cdot \nabla_y \chi^1$ might seem to be of the same order, but

- since u° vanishes on Γ, $u^\circ \approx \varepsilon(\partial u_1^\circ/\partial x_2)(x_1, 0)(x_2/\varepsilon)$.
- $\nabla_y \chi^1$ decays exponentially fast as x_2/ε goes to infinity.

Thus the two factors compensate and the convective term is actually smaller.

Therefore, χ^1 and π^1 have to be chosen so that

$$-\mu \Delta_y \chi^1 + \nabla_y \pi^1 = 0. \tag{17}$$

In the same manner,

$$\nabla \cdot \left(u^\circ + \varepsilon u_{BL}^1\right) = \frac{\partial u_1^\circ}{\partial x_2}(x_1, 0)\nabla_y \cdot \chi^1 + \varepsilon \frac{\partial^2 u_1^\circ}{\partial x_2 \partial x_1}(x_1, 0)\chi_1^1 + \text{smaller order terms.} \tag{18}$$

The leading order term in (18) is $(\partial u_1^\circ/\partial x_2)(x_1, 0)\nabla_y \cdot \chi^1$; therefore, χ^1 must satisfy

$$\nabla_y \cdot \chi^1 = 0. \tag{19}$$

There remains to look at the boundary condition on Γ^ε:

$$u^\circ + \varepsilon u^1_{BL} = \varepsilon\left(\frac{x_2}{\varepsilon}e_1 + \chi^1\left(\frac{x}{\varepsilon}\right) - \langle\chi^1\rangle\right)\frac{\partial u_1^\circ}{\partial x_2}(x_1, 0) + \text{smaller order terms} \tag{20}$$

on Γ^ε. From (20), it is very tempting to impose that

$$\chi^1(y) - \langle\chi^1\rangle = -y_2\, e_1 \quad \text{on } \partial Y_3 \cup \partial Y_4.$$

However, with this condition, the problem satisfied by $(\chi^1(y) - \langle\chi^1\rangle, \pi^1(y))$ becomes

$$\begin{aligned} -\mu\Delta_y(\chi^1 - \langle\chi^1\rangle) + \nabla_y\pi^1 &= 0 && \text{in } Y,\\ \nabla_y\cdot(\chi^1 - \langle\chi^1\rangle) &= 0 && \text{in } Y,\\ \chi^1 - \langle\chi^1\rangle &= -y_2\, e_1 && \text{on } \partial Y_3 \cup \partial Y_4,\\ \chi^1 - \langle\chi^1\rangle &\in \mathcal{S}^2_{\text{per}},\\ \pi^1 &\in \mathcal{S}_{\text{per}}. \end{aligned} \tag{21}$$

It can be proved by taking, for example, the very simple case where $\partial Y_4 = (0, 2\pi)\times\{y_2 = C > 0\}$ (the problems becomes 1D) that this problem has, in general, no solutions. Therefore, we have to relax the boundary condition on Γ^ε, and we impose that

$$\chi^1 = -y_2\, e_1 \quad \text{on } \partial Y_3 \cup \partial Y_4, \tag{22}$$

and the error on Γ^ε is

$$u^\circ + \varepsilon u^1_{BL} = -\varepsilon\langle\chi^1\rangle\frac{\partial u_1^\circ}{\partial x_2}(x_1, 0) + \text{smaller order terms.} \tag{23}$$

It seems from (23) that if $\langle\chi^1\rangle \neq 0$, no progress has been made by adding εu^1_{BL} to u°, since the error on the no-slip condition on Γ^ε is of the same order. However, a closer inspection of (23) shows that the error at leading order no longer depends on the fast variable x/ε. Therefore, this error can be corrected by replacing (u°, p°) by (u^1, p^1), where u^1 and p^1 do not depend on x/ε (see Step 5 below).

Step 4. We can now write the problem satisfied by $(\chi^1, \langle\chi^1\rangle, \pi^1)$:

$$\begin{aligned} -\mu\Delta_y\chi^1 + \nabla_y\pi^1 &= 0 && \text{in } Y,\\ \nabla_y\cdot\chi^1 &= 0 && \text{in } Y,\\ \chi^1 &= -y_2\, e_1 && \text{on } \partial Y_3 \cup \partial Y_4,\\ \chi^1 - \langle\chi^1\rangle &\in \mathcal{S}^2_{\text{per}},\\ \pi^1 &\in \mathcal{S}_{\text{per}}. \end{aligned} \tag{24}$$

Let us introduce the space $L^2_{\text{per}}(Y)$ of the functions in Y, 2π-periodic in the y_1 variable, and square integrable in Y, and the space $H^1_{\text{per}}(Y) \subset L^2_{\text{per}}(Y)$ of the functions whose first derivatives belong to $L^2_{\text{per}}(Y)$. We have the following result.

THEOREM 3.1. *There exist a unique pair of functions* (χ^1, π^1) *and a unique vector* $\langle\chi^1\rangle \in \mathbb{R}^2$ *such that* $\chi^1 - \langle\chi^1\rangle \in H^1_{\text{per}}{}^2(Y) \cap \mathcal{S}^2_{\text{per}}(Y)$, $\pi^1 \in L^2_{\text{per}}(Y) \cap \mathcal{S}_{\text{per}}(Y)$, *and* (24) *is satisfied in a weak-sense. Moreover,* $\langle\chi^1\rangle$ *is horizontal*:

$$\langle\chi^1\rangle = \overline{\chi^1} e_1.$$

This theorem will be proved in Section 6.1.

Step 5. There remains to correct the error in (23) by replacing (u°, p°) by (u^1, p^1) solutions of the same Navier–Stokes problem with the new boundary condition on Γ,

$$\begin{aligned} u^1 \cdot \nabla u^1 - \mu\varepsilon\Delta u^1 + \nabla p^1 &= f && \text{in } \Omega^\circ, \\ \nabla \cdot u^1 &= 0 && \text{in } \Omega^\circ, \\ u^1 &= 0 && \text{on } \partial\Omega^\circ \backslash \Gamma, \\ u^1 &= \varepsilon\langle\chi^1\rangle \frac{\partial u_1^\circ}{\partial x_2} && \text{on } \Gamma. \end{aligned} \tag{25}$$

We have constructed $(u^1(x) + \varepsilon u^1_{BL}(x, x/\varepsilon),\ p^1(x) + \varepsilon p^1_{BL}(x, x/\varepsilon))$ approximating $(u^\varepsilon, p^\varepsilon)$. It can be proved (at least in the linear case; see [1, 2, 4]) that this approximation is one order (in $\sqrt{\varepsilon}$) better than (u°, p°), but it is not the purpose of this paper.

Remark 3.2. In order to avoid discontinuities at the transition between the rough and flat walls, it may be better to take

$$u^1_{BL}\left(x, \frac{x}{\varepsilon}\right) = \frac{\partial u_1^\circ}{\partial x_2}(x_1, 0)\left(\chi^1\left(\frac{x}{\varepsilon}\right) - \overline{\chi^1} e_1\right)\phi(x_1),$$

$$p^1_{BL}\left(x, \frac{x}{\varepsilon}\right) = \frac{\partial u_1^\circ}{\partial x_2}(x_1, 0)\pi^1\left(\frac{x}{\varepsilon}\right)\phi(x_1),$$

where $\phi(x_1)$ is a real smooth function taking the value 1 in the interval $(\gamma_1 + \varepsilon, \gamma_2 - \varepsilon)$, 0 in $(-\infty, \gamma_1) \cap (\gamma_2, +\infty)$, and with the derivative bounded by C/ε. Thus the boundary layer correctors vanish smoothly at the transition zones between the rough and smooth boundaries. With this choice of boundary layer correctors and the functions (u^1, p^1) defined in (25), the functions $u^1 + \varepsilon u^1_{BL}$, $p^1 + \varepsilon p^1_{BL}$ plugged into (5) produce also an error localized to the transition zone, which can be neglected at this order of approximation, since we are interested in energy norms.

Step 6 (*The effective boundary conditions*). In practice, computing (u°, p°) and then (u^1, p^1) consists of solving two Navier–Stokes problems in Ω°, which is too expensive. A better idea is to notice that near Γ, $u^1 \approx u^\circ$, and that the boundary condition (25) on Γ can be replaced by the Navier boundary condition,

$$u^1 = \varepsilon\langle\chi^1\rangle \frac{\partial u_1^1}{\partial x_2} \quad \text{on } \Gamma. \tag{26}$$

If $\overline{\chi^1} \neq 0$, the boundary value problem becomes

$$\begin{aligned} u^1 \cdot \nabla u^1 - \mu\varepsilon \Delta u^1 + \nabla p^1 &= f, \quad \text{in } \Omega^\circ, \\ \nabla \cdot u^1 &= 0, \quad \text{in } \Omega^\circ, \\ u^1 &= 0, \quad \text{on } \partial\Omega^\circ \backslash \Gamma, \\ \varepsilon\mu \frac{\partial u_1^1}{\partial n} + \frac{\mu}{\chi^1} u_1^1 &= 0, \quad \text{on } \Gamma, \\ u_2^1 &= 0, \quad \text{on } \Gamma. \end{aligned} \tag{27}$$

However, (27) may be ill posed if the constant $\overline{\chi^1}$ is negative due to the loss of ellipticity, because its variational formulation contains the term

$$\frac{\mu}{\overline{\chi^1}} \int_\Gamma u_1^1 v_1.$$

To cure this problem, we introduce Ω^δ given by (9) and we solve (27) in Ω^δ rather than in Ω°. A Taylor expansion on u°,

$$\begin{aligned} u^\circ(x_1, 0) &= u^\circ(x_1, \varepsilon\delta) - \varepsilon\delta \frac{\partial u^\circ}{\partial x_2}(x_1, \varepsilon\delta) + \frac{\varepsilon^2\delta^2}{2} \frac{\partial^2 u^\circ}{\partial x_2^2}(x_1, \theta\varepsilon\delta), \\ \frac{\partial u^\circ}{\partial x_2}(x_1, \varepsilon\delta) &= \frac{\partial u^\circ}{\partial x_2}(x_1, 0) + \varepsilon\delta \frac{\partial^2 u^\circ}{\partial x_2^2}(x_1, \theta'\varepsilon\delta), \end{aligned} \tag{28}$$

combined with the incompressibility condition shows that

$$\begin{aligned} &\varepsilon\mu \frac{\partial u_1^1}{\partial n} + \frac{\mu}{\overline{\chi^1}} u_1^1 = 0, \quad u_2^1 = 0 \quad \text{on } \Gamma, \\ \Rightarrow \quad &\varepsilon\mu \frac{\partial u_1^1}{\partial n} + \frac{\mu}{\overline{\chi^1} + \delta} u_1^1 = 0, \quad u_2^1 = 0 \quad \text{on } \Gamma^\delta, \end{aligned}$$

up to smaller order terms. This is the effective boundary condition on Γ^δ given in (11).

3.4. *Bounds on the Constant* $\overline{\chi^1}$

From a Taylor expansion analogous to (14), it can be seen that the first-order effective condition is equivalent to a no-slip condition at the effective height $-\varepsilon\overline{\chi^1}$. Thus, the ansatz above is nothing else but the rigorous computation of an effective wall, equivalent at first order to the rough wall, which cannot be foreseen otherwise.

One may ask the question: is it possible to bound the effective height $-\varepsilon\overline{\chi^1}$? It is reasonable to expect that $-\overline{\chi^1}$ is bounded from below by 0 (the minimal value of y_2 in ∂Y) and from above by the amplitude of the roughness (the maximal value of y_2 in $\partial Y_3 \cup \partial Y_4$). Indeed, this is true, as will be proved in Section 6.2.

THEOREM 3.2. *If* $H_{\max} = \max_{y \in \partial Y_4 \cup \partial Y_3} y_2$, *the constant* $-\overline{\chi^1}$ *satisfies the bound*

$$0 \leq -\overline{\chi^1} \leq H_{\max}. \tag{29}$$

4. THE SECOND-ORDER EFFECTIVE BOUNDARY CONDITION

Here, we propose to carry out the ansatz one step further. We are going to obtain a second boundary condition which will take into account some convection effects.

4.1. *The Second-Order Effective Boundary Conditions: The Practical Implementation*

We propose to approximate $(u^\varepsilon, p^\varepsilon)$ in Ω^δ by (u^2, p^2) the solution of the Navier–Stokes problem,

$$\begin{aligned} u^2 \cdot \nabla u^2 - \mu\varepsilon \Delta u^2 + \nabla p^2 &= f, \quad \text{in } \Omega^\delta, \\ \nabla \cdot u^2 &= 0, \quad \text{in } \Omega^\delta, \\ u^2 &= 0, \quad \text{on } \partial\Omega^\delta \backslash \Gamma^\delta, \end{aligned} \tag{30}$$

with the nonlinear second-order effective boundary condition on Γ^δ,

$$\begin{gathered} \varepsilon\mu \frac{\partial u_1^2}{\partial n} + \frac{\mu}{\overline{\chi^1} + \delta} u_1^2 + \frac{1}{\overline{\chi^1} + \delta} \left(-\varepsilon \left(\delta \overline{\chi^1} + \frac{\delta^2}{2} - \overline{\chi^3} \right) \frac{\partial p^2}{\partial x_1} - \mu \frac{\overline{\chi^2}}{(\overline{\chi^1} + \delta)^2} \left(u_1^2\right)^2 \right) = 0, \\ u_2^2 = 0, \end{gathered} \tag{31}$$

where u_1^2, u_2^2 are the two components of u^2. Here $\overline{\chi^1}$ is given by (12), and the other two constants $\overline{\chi^2}$ and $\overline{\chi^3}$ are computed by solving the cell problems in Y:

1. find the velocity field χ^2 and the pressure field π^2 defined in Y, and find the constant parameter $\overline{\chi^2}$ such that

$$\begin{aligned} -\mu \Delta \chi^2 + \nabla \pi^2 &= -\left(y_2\, e_1 \cdot \nabla \chi^1 + \chi_2^1 e_1 + \chi^1 \cdot \nabla \chi^1 \right), \quad \text{in } Y, \\ \nabla \cdot \chi^2 &= 0, \quad \text{in } Y, \\ \chi^2 &= 0, \quad \text{on } \partial Y_3 \cup \partial Y_4, \\ \chi^2 - \overline{\chi^2}\, e_1 &\in \mathcal{S}_{\text{per}}^2, \\ \pi^2 &\in \mathcal{S}_{\text{per}}. \end{aligned} \tag{32}$$

2. find the velocity field χ^3 and the pressure field π^3 defined in Y, and find the constant parameter $\overline{\chi^3}$ such that

$$\begin{aligned} -\mu \Delta \chi^3 + \nabla \pi^3 &= 0, \quad \text{in } Y, \\ \nabla \cdot \chi^3 &= 0, \quad \text{in } Y, \\ \chi^3 &= -\frac{y_2^2}{2}\, e_1, \quad \text{on } \partial Y_3 \cap \partial Y_4, \\ \chi^3 - \overline{\chi^3}\, e_1 &\in \mathcal{S}_{\text{per}}^2, \\ \pi^3 &\in \mathcal{S}_{\text{per}}. \end{aligned} \tag{33}$$

To summarize, in order to compute the approximation (u^2, p^2) of $(u^\varepsilon, p^\varepsilon)$, the algorithm is the following:

1. approximate numerically the solutions of the three cell problems (12), then (32) and (33) by a finite element method, for example;
2. solve the Navier–Stokes problem (30), (31) in the domain Ω^δ.

4.2. *The Ansatz*

In order to improve the approximation of u^ε and p^ε, we propose the ansatz

$$\begin{aligned} u^\varepsilon(x) &\approx u^2(x) + \varepsilon u^1_{BL}\left(x, \frac{x}{\varepsilon}\right) + \varepsilon^2 u^2_{BL}\left(x, \frac{x}{\varepsilon}\right), \\ p^\varepsilon(x) &\approx p^2(x) + \varepsilon p^1_{BL}\left(x, \frac{x}{\varepsilon}\right) + \varepsilon^2 p^2_{BL}\left(x, \frac{x}{\varepsilon}\right), \end{aligned} \tag{34}$$

where the first-order boundary layer terms have already been computed. We carry out the same steps as in Section 3.3.

Let us evaluate the error made when we plug $u^1 + \varepsilon u^1_{BL}$, $p^1 + \varepsilon p^1_{BL}$ in (5). To compute $\mathcal{L}^\varepsilon(u^1 + \varepsilon u^1_{BL},\ p^1 + \varepsilon p^1_{BL})$ at leading order, we need to know, at leading order, the three following terms:

$$u^1 \cdot \nabla u^1_{BL} \approx \varepsilon \left(\frac{\partial u^1_1}{\partial x_2}\right)^2 (x_1, 0)\left(\langle \chi^1 \rangle + y_2\, e_1\right) \cdot \nabla_y \chi^1\left(\frac{x}{\varepsilon}\right);$$

$$u^1_{BL} \cdot \nabla u^1 = \frac{\partial u^1_1}{\partial x_2}(x_1, 0)\left(\chi^1\left(\frac{x}{\varepsilon}\right) - \langle \chi^1 \rangle\right) \cdot \nabla_x u^1 \approx \left(\frac{\partial u^1_1}{\partial x_2}\right)^2 (x_1, 0)\chi^1_2\left(\frac{x}{\varepsilon}\right) e_1;$$

$$u^1_{BL} \cdot \nabla u^1_{BL} \approx \frac{1}{\varepsilon}\left(\frac{\partial u^1_1}{\partial x_2}\right)^2 (x_1, 0)\left(\chi^1\left(\frac{x}{\varepsilon}\right) - \langle \chi^1 \rangle\right) \cdot \nabla_y \chi^1\left(\frac{x}{\varepsilon}\right).$$

Therefore, the leading order term of $\mathcal{L}^\varepsilon(u^1 + \varepsilon u^1_{BL},\ p^1 + \varepsilon p^1_{BL})$ is

$$\begin{aligned} &\mathcal{L}^\varepsilon\left(u^1 + \varepsilon u^1_{BL},\ p^1 + \varepsilon p^1_{BL}\right) \\ &\quad = \varepsilon \left(\frac{\partial u^1_1}{\partial x_2}\right)^2 (x_1, 0)\left(y_2\, e_1 \cdot \nabla_y \chi^1\left(\frac{x}{\varepsilon}\right) + \chi^1_2\left(\frac{x}{\varepsilon}\right) e_1 + \chi^1\left(\frac{x}{\varepsilon}\right) \cdot \nabla_y \chi^1\left(\frac{x}{\varepsilon}\right)\right) \\ &\qquad + \text{smaller order terms.} \end{aligned} \tag{35}$$

In the same manner, the error on the divergence-free condition is

$$\nabla \cdot \left(u^1 + \varepsilon u^1_{BL}\right) = \varepsilon \frac{\partial^2 u^\circ_1}{\partial x_2 \partial x_1}(x_1, 0)\left(\chi^1 \cdot e_1 - \overline{\chi^1}\right) + \text{smaller order terms.}$$

Since $|(\partial^2 u^\circ_1/\partial x_2 \partial x_1)(x_1, 0)| \ll |(\partial u^1_1/\partial x_2)(x_1, 0)|$, this error need not be corrected at leading order.

The error on the boundary condition on Γ^ε is at leading order

$$\left(u^1 + \varepsilon u^1_{BL}\right) \approx \frac{x_2^2}{2} \frac{\partial^2 u^1_1}{\partial x_2^2}(x_1, 0)\, e_1 \quad \text{on } \Gamma^\varepsilon. \tag{36}$$

As in Section 3.3, we notice that the errors in (35) and (36) are the products of fast oscillating periodic terms by slow varying functions, namely $\varepsilon(\partial u^1_1/\partial x_2)^2(x_1, 0)$ and $(\partial^2 u^1_1/\partial x_2^2)(x_1, 0)$.

Therefore, it is natural to look for correctors of the form

$$u^2_{BL}(x) = \left(\chi^2\left(\frac{x}{\varepsilon}\right) - \overline{\chi^2}\, e_1\right)\left(\frac{\partial u^1_1}{\partial x_2}\right)^2(x_1,0) + \left(\chi^3\left(\frac{x}{\varepsilon}\right) - \overline{\chi^3}\, e_1\right)\frac{\partial^2 u^1_1}{\partial x_2^2}(x_1,0),$$
$$p^2_{BL}(x) = \pi^2\left(\frac{x}{\varepsilon}\right)\left(\frac{\partial u^1_1}{\partial x_2}\right)^2(x_1,0) + \pi^3\left(\frac{x}{\varepsilon}\right)\frac{\partial^2 u^1_1}{\partial x_2^2}(x_1,0), \tag{37}$$

where χ^2, χ^3 (resp. π^2, π^3) are functions with value in $\mathbb{R}^2$ (resp. $\mathbb{R}$), periodic in the y_1 direction, and $\overline{\chi^2}$, $\overline{\chi^3}$ are two constant parameters. We impose further that $\chi^2 - \overline{\chi^2}\, e_1$, $\chi^3 - \overline{\chi^3}\, e_1$, π^2, and π^3, as well as all their derivatives, decay exponentially fast as y_2 goes to infinity.

Exactly, as in Sections 3.3, we see from (34), (35) that $(\chi^2, \pi^2, \overline{\chi^2})$ should satisfy (32) and that $(\chi^3, \pi^3, \overline{\chi^3})$ should satify (33). The existence and uniqueness of the solutions of (32) and (33) can be proved as for Theorem 3.1.

Exactly as in Section 3, we find that the errors in (34), (35) are corrected by the boundary layer terms defined in (37), except that there remains an error on the no-slip condition on Γ^ε, namely

$$-\varepsilon^2\left(\overline{\chi^2}\left(\frac{\partial u^1_1}{\partial x_2}\right)^2 + \overline{\chi^3}\frac{\partial^2 u^1_1}{\partial x_2^2}\right)e_1,$$

which no longer depends on the fast variable x/ε. To correct it, we introduce the second-order macroscopic corrections (u^2, p^2) satisfying the Navier–Stokes equations in Ω° with the new second-order effective boundary conditions on Γ,

$$u^2 = \varepsilon\overline{\chi^1}\frac{\partial u^1_1}{\partial x_2}\, e_1 + \varepsilon^2\left(\overline{\chi^2}\left(\frac{\partial u^1_1}{\partial x_2}\right)^2 + \overline{\chi^3}\frac{\partial^2 u^1_1}{\partial x_2^2}\right)e_1 \quad \text{on } \Gamma. \tag{38}$$

Remark 4.1. Here, we have neglected the contribution of the limiting function ϕ introduced in Remark 3.2. In fact, the error produced by this function is in L^2-norm of the same order as the error computed in (35), but it is localized in a zone of diameter $O(\varepsilon)$. For a complete analysis, this error term should also be corrected. The related corrector depends on the fast variable x/ε and decays (but not exponentially) away from the transition zone. Since it remains localized in a region of small size, it can be neglected if we are interested in a second-order approximation of the flow far enough from the wall.

The related effective conditions. As in Section 3, it is more convenient to compute (u^2, p^2) by changing slightly the boundary conditions (38) on Γ. Indeed, one may use the second-order effective boundary conditions

$$u^2 = \varepsilon\overline{\chi^1}\frac{\partial u^2}{\partial x_2}\, e_1 + \varepsilon^2\left(\overline{\chi^2}\left(\frac{\partial u^2_1}{\partial x_2}\right)^2 + \overline{\chi^3}\frac{\partial^2 u^2_1}{\partial x_2^2}\right)e_1 \quad \text{on } \Gamma. \tag{39}$$

Note that the boundary condition (39) is nonlinear. In order to simplify the notations, we set

$$u = u^2, \quad p = p^2$$

for the rest of this section.

If $\overline{\chi^1} \neq 0$, (39) can be written in a more handy form,

$$u_2 = 0, \quad \varepsilon\mu \frac{\partial u_1}{\partial n} + \frac{\mu}{\overline{\chi^1}} u_1 - \frac{\mu}{\overline{\chi^1}} \varepsilon^2 \left(\overline{\chi^2} \left(\frac{\partial u_1}{\partial x_2} \right)^2 + \overline{\chi^3} \frac{\partial^2 u_1}{\partial x_2^2} \right) = 0,$$

where the subscripts indicate the coordinates.

Moreover, by using the first-order approximation of $\partial u_1/\partial x_2$ given by (25), $(\mu/\overline{\chi^1})\varepsilon^2 \overline{\chi^2} (\partial u_1/\partial x_2)^2$ can be replaced by $\mu(\overline{\chi^2}/\overline{\chi^1}^3)(u_1)^2$. With this trick, we avoid having the nonlinearity on a derivative.

Furthermore, the Navier–Stokes equations on the boundary indicate that at leading order:

$$\mu\varepsilon \frac{\partial^2 u_1}{\partial x_2^2}(x_1, 0) \approx \frac{\partial p}{\partial x_1}(x_1, 0).$$

Therefore, it is possible to obtain the set of boundary conditions:

$$u_2 = 0, \quad \varepsilon\mu \frac{\partial u_1}{\partial n} + \frac{\mu}{\overline{\chi^1}} u_1 + \varepsilon \frac{\overline{\chi^3}}{\overline{\chi^1}} \frac{\partial p}{\partial x_1} - \mu \frac{\overline{\chi^2}}{\overline{\chi^1}^3} (u_1)^2 = 0.$$

As for the first-order approximation, the boundary value problem in Ω° may be ill posed. However, it is possible to construct a well-posed problem in the domain Ω^δ defined in Section 3.1. From a Taylor expansion, we obtain that

$$\begin{aligned}
u_1(x_1, 0) &= u_1(x_1, \varepsilon\delta) - \varepsilon\delta \frac{\partial u_1}{\partial x_2}(x_1, \varepsilon\delta) + \frac{\varepsilon^2\delta^2}{2} \frac{\partial^2 u_1}{\partial x_2^2}(x_1, \varepsilon\delta) + O(\varepsilon^3\delta^3), \\
\frac{\partial u_1}{\partial x_2}(x_1, 0) &= \frac{\partial u_1}{\partial x_2}(x_1, \varepsilon\delta) - \varepsilon\delta \frac{\partial^2 u_1}{\partial x_2^2}(x_1, \varepsilon\delta) + O(\varepsilon^2\delta^2), \\
\left(\frac{\partial u_1}{\partial x_2} \right)^2 (x_1, 0) &= \left(\frac{\partial u_1}{\partial x_2} \right)^2 (x_1, \varepsilon\delta) + O(\varepsilon\delta).
\end{aligned}$$

Thus, the effective second-order boundary conditions on Γ^δ are

$$\begin{gathered}
u_2 = 0, \\
\varepsilon\mu \frac{\partial u_1}{\partial n} + \frac{\mu}{\overline{\chi^1} + \delta} u_1 + \varepsilon^2 \frac{\mu}{\overline{\chi^1} + \delta} \left(\left(\delta\overline{\chi^1} + \frac{\delta^2}{2} - \overline{\chi^3} \right) \frac{\partial^2 u_1}{\partial n^2} - \overline{\chi^2} \left(\frac{\partial u_1}{\partial n} \right)^2 \right) = 0,
\end{gathered}$$

or, again,

$$\begin{gathered}
u_2 = 0, \\
\varepsilon\mu \frac{\partial u_1}{\partial n} + \frac{\mu}{\overline{\chi^1} + \delta} u_1 + \frac{1}{\overline{\chi^1} + \delta} \left(-\varepsilon \left(\delta\overline{\chi^1} + \frac{\delta^2}{2} - \overline{\chi^3} \right) \frac{\partial p}{\partial x_1} - \mu \frac{\overline{\chi^2}}{(\overline{\chi^1} + \delta)^2} (u_1)^2 \right) = 0,
\end{gathered} \tag{40}$$

and we obtain (30).

In the two sets of boundary conditions above, we have neglected the corrections from the Taylor expansion of u_2, because they are of a smaller order.

Remark 4.2. We have seen in Section 3.4 that the first-order condition is equivalent to a no-slip condition on a flat wall at height $-\varepsilon\overline{\chi^1}$. This is not the case in general for the second-order effective conditions.

5. NUMERICAL VALIDATION

5.1. *General Features*

The numerical validation is done with a 2D steady-state Navier–Stokes code. The discretization is done by means of stabilized isoparametric $Q_1 - Q_1$ elements; we use a mesh composed of quadrangular elements. For each quadrangle Q of the mesh, the unit square may be mapped to Q by a simple transformation T_Q, linear with respect to each coordinate. Both the pressure and the velocity components are discretized in the space of continuous functions v_h satisfying the following property; for any element Q, the function $v_h \circ T_Q$ defined on the unit square is linear with respect to each coordinate.

However, using a straightforward Galerkin method with the same spaces for the pressure and the velocity components is well known to lead to an unstable discretization of (5) as the discretized pressure can have spurious oscillating modes (checker board instabilities [12]). The remedy for that is to *stabilize* the method, by adding suitably weighted element-wise residuals to the original variational formulation. These residuals may be constructed by taking in each element the least square formulation of (5) (see [10, 19]).

The nonlinear discrete problem is solved with a Newton method. A single step of the Newton method involves solving a nonsymetric linear system here with a GMRES algorithm [16].

The direct solution of (5) with the no-slip condition on the rough wall Γ^ε is computed with high accuracy, i.e. with a large number of elements. It is compared with:

1. The solution of (7) with a no-slip condition on Γ and with the domain of computation Ω° (the boundary condition is referred to as the zeroth-order wall law). As for the next two problems, the mesh may be much coarser than for the direct computation.
2. The solution of problem (11) with the first-order effective boundary condition on the smooth wall $x_2 = \delta\varepsilon$.
3. The solution of problem (30) with the second-order effective boundary condition on the smooth wall $x_2 = \delta\varepsilon$.

For problems (11) and (30), the effective boundary condition has not been imposed on Γ but at $x_2 = \delta\varepsilon$. The new domain has steps at $x_1 = \gamma_1$ and $x_1 = \gamma_2$ because x_2 jumps from 0 to $\delta\varepsilon$. These singularities of the domain are natural, since the solution of the effective problems are singular at $x_1 = \gamma_1$ and $x_1 = \gamma_2$. The choice of δ is clearly an issue of the proposed method; indeed, δ should be large enough so that the effective problem is well posed and small enough so that the line $x_2 = \delta\varepsilon$ is contained in the mean flow laminar boundary layer.

We have also tried the effective first and second conditions on Γ, (26) and (39), but this leads to linearized systems with very small Gauss pivots, and the corresponding solution strongly oscillates near the wall.

In the tests below, the wall is made of one piece; i.e., the set ∂Y_4 is empty.

For the last two procedures, the linear Stokes cell problems (24), then (32) and (33) need to be solved. The cells are artificially truncated in the y_2-direction and are limited by a section $\partial Y_H : y_2 = H$ with H large enough. In practice, since the solutions converge very

fast as y_2 grows, H can be chosen 5 to 20 times the size of the roughness element. The cell problems involve:

1. periodic boundary conditions on the velocity and the pressure on ∂Y_1-∂Y_2. Periodicity is crucial to obtain the fast decay of the solution as y_2 grows and need to be imposed with accuracy. If the periodicity was not achieved, the Fourier modes in y_1 would not be well separated, and the exponential convergence to a constant as $y_2 \to \infty$ would not hold.

2. an artificial boundary condition on ∂Y_H. It is possible to impose an exactly transparent integro-differential boundary condition for χ^1, π^1 and χ^2, π^2 by using the Fourier analysis of 6.1. However, it has proved sufficient to take an homogeneous Neumann condition (resp. Dirichlet condition) for the first (resp. second) component of the velocity; for example,

$$\frac{\partial}{\partial n}\chi_1^1 = 0, \quad \chi_2^1 = 0 \quad \text{on } \partial Y_H.$$

The values of the constants $\overline{\chi^1}$, $\overline{\chi^2}$, and $\overline{\chi^3}$ are computed by taking the mean value of the corresponding velocities on ∂Y_H.

The cell problems do not need a very fine mesh. The corresponding linear systems are solved by means of a direct method (Gauss factorization).

The comparison between the different solutions are done on several outputs:

1. the contour lines of the velocity components or the pressure. For comparing the four solutions, the same contour lines are displayed on the different figures. This is made possible by the INRIA graphic package VIGIE [9].

2. the restriction of the horizontal velocity u_1 on a given horizontal cross section above the rough wall.

3. the friction $C_f = \mu\varepsilon(\partial u_1/x_2)$ on the same horizontal cross section.

5.2. *Flat Plate with Nonsymmetric Roughness*

The domain Ω° is $(0, 1.0) \times (0, 0.5)$. The plate is located on the axis $x_2 = 0$. The plate is flat in the interval $0 < x_1 < 0.18$ and has periodic roughness in the interval $0.18 < x_1 < 1.0$. The period of the roughness elements is 0.05 and their maximal height is 0.025. The rough domain can be seen on Fig. 5.

A no-slip condition is imposed on the wall $x_2 = 0.5$. At the inflow boundary $x_1 = 0$, the velocity is set to a developed profile of velocity on a flat plate. The viscosity is taken to be 10^{-3}. We choose $\mu = 0.04$ and $\varepsilon = 0.025$.

At the outflow boundary $x_1 = 1.0$, an homogeneous Neumann (resp. Dirichlet) condition is imposed on the first (resp. second) component of the velocity.

The horizontal size of the cell Y is 2, and the cell is artificially truncated at $y_2 = 5$. The amplitude of the roughness element is 1 in the microscopic variables. The mesh for the cell problems has 2500 elements.

The values of the computed constants are

$$\overline{\chi^1} = -0.84, \quad \overline{\chi^2} = 2.6 \times 10^{-4}, \quad \overline{\chi^3} = -0.36.$$

Note that the mean value of y_2 on ∂Y_3 is 0.25, which is much less than the effective heigth $-\overline{\chi^1} = 0.84$.

For the first- and second-order effective boundary value problems,the wall law is imposed on the line $x_2 = \delta = 0.025$. Figure 4 contains the contour lines of respectively χ_1^1, χ_1^2, and χ_1^3,

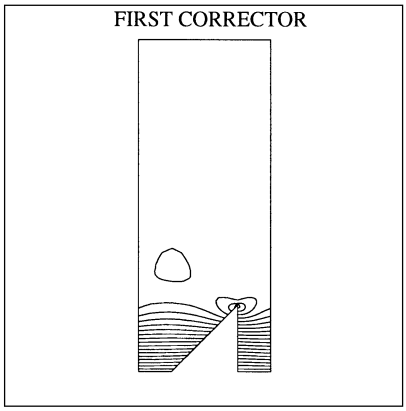

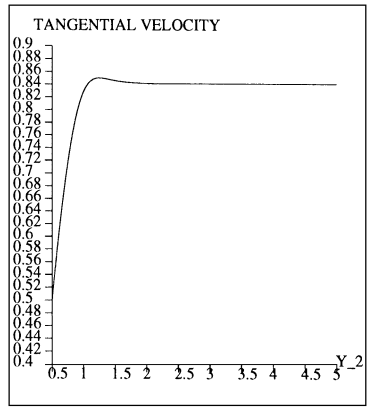

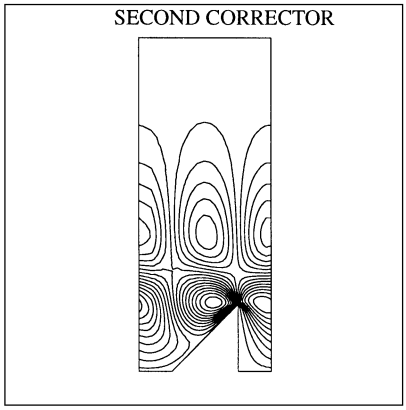

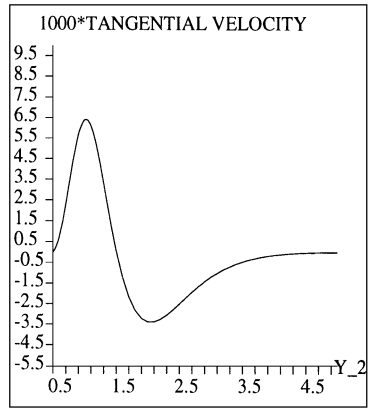

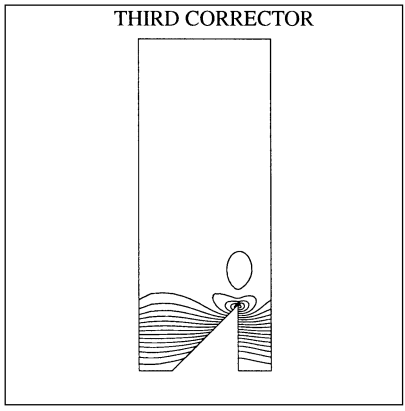

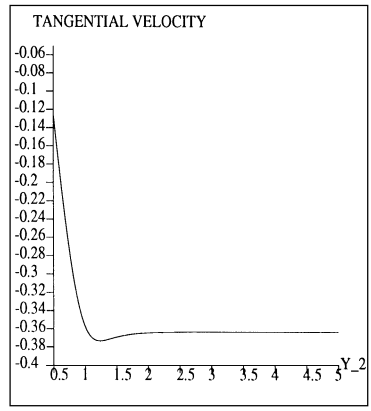

FIG. 4. Contour lines of χ_1^1, χ_1^2, and χ_1^3 for the nonsymmetric roughness and cross sections $y_2 = 1$.

as well as a plot of their value on the cross section $y_1 = 1$. The convergence to constant values appears clearly. On Fig. 5, we display the horizontal velocity for the direct solution and the three approximations of u^ε listed above. It is clear that the roughness elements lie within the boundary layer of the mean flow: therefore, the asymptotic expansion above is sensible. On this figure, the difference between the four computed solutions is not easily seen. A zoom (Fig. 6) indicates that there are important recirculations in the cavities delimited by the rough wall.

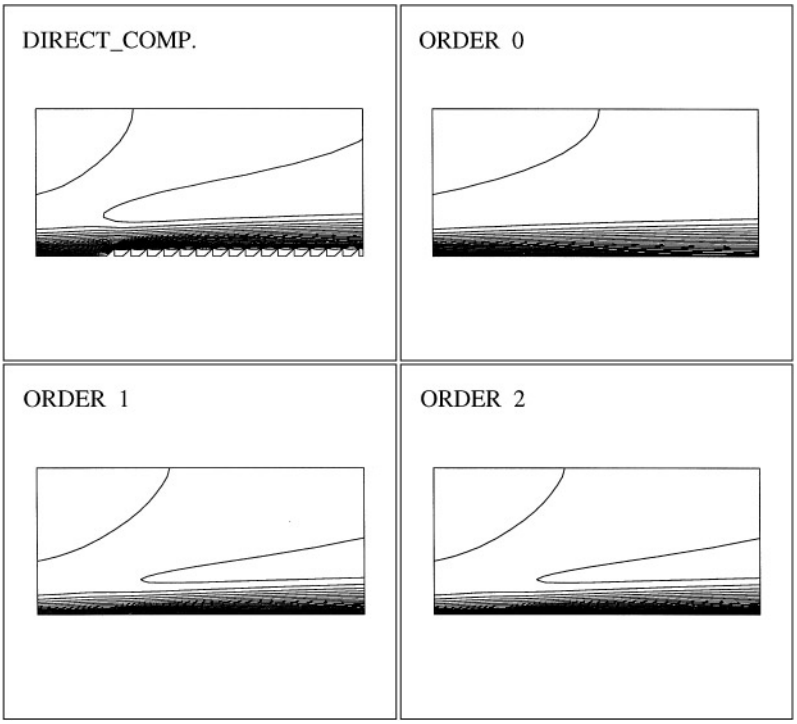

FIG. 5. The horizontal velocity for the four Navier–Stokes problems.

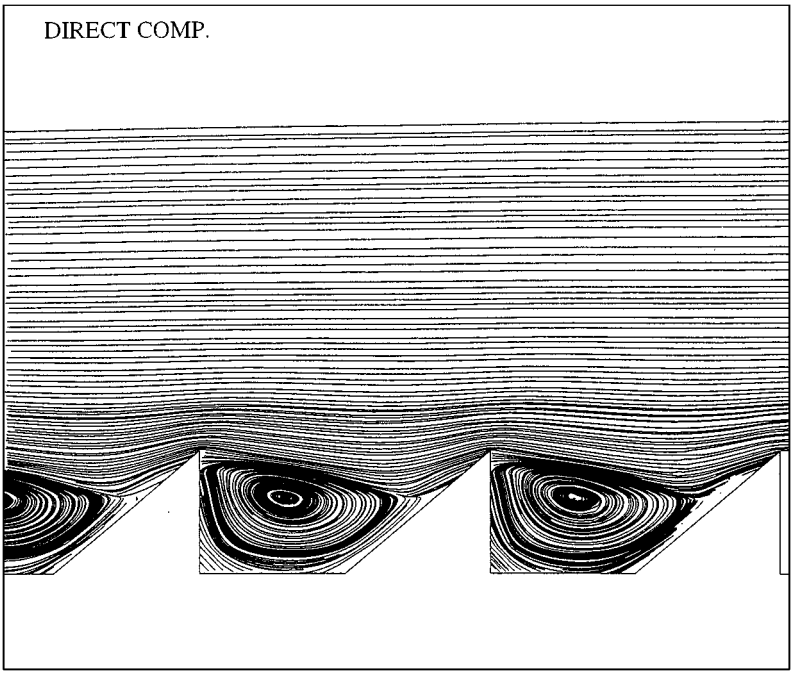

FIG. 6. Zoom in one roughness element.

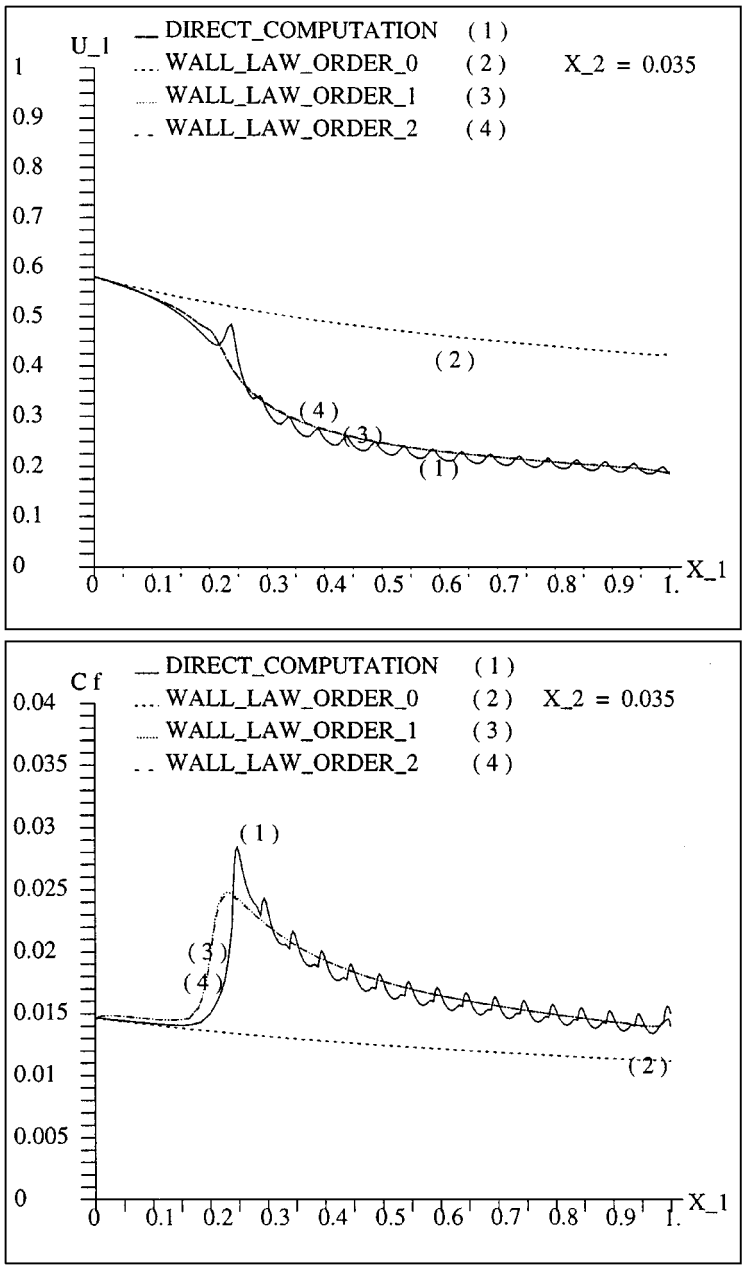

FIG. 7. u_1 (up) and $C_f = \mu\varepsilon(\partial u_1/x_2)$ (bottom) on the cross section $x_2 = 0.035$.

On Fig. 7, we present the horizontal component of the velocity u_1 and the coefficient C_f on the cross section $x_2 = 0.035$. Figure 7 clearly indicates that the effective boundary conditions yield a remarkably accurate approximation of the exact solution, while the no-slip boundary condition on Γ is not sufficient. As expected, the error remains important in the transition zone between the flat and the rough parts, but decays fast in the rough zone. In principle, this error may be addressed by an additional corrector, which would not be as local as χ^1, χ^2, and χ^3 and, thus, would be much more difficult to compute.

It is not clear here that the second-order effective conditions do better than the first order ones.

5.3. *Flow in a Channel with Two Kinds of Roughness*

This test is concerned with a flow in a channel. The domain Ω° is $(0, 1.0) \times (0, 0.5)$. The bottom boundary is flat in the intervals (0, 0.25), has nonsymmetric periodic roughness in the interval (0.25, 0.75), and has sinusoidal periodic roughness in the interval (0.75, 1). The nonsymmetric roughness is the same as in 5.2. The period of the sinusoidal roughness is 0.04 and the amplitude is 0.01.

A no-slip condition is imposed on the wall $x_2 = 0.5$ and at the bottom boundary. A parabolic profile is imposed at the entry of the channel. The boundary conditions at $x_1 = 1$ are $u_2 = 0$ and $p = 0$.

The viscosity is taken to be 10^{-2}. We choose to take $\mu = 0.4$ and $\varepsilon = 0.025$.

The direct computation is done with 12000 elements. Refinement is needed near the rough wall, simply to take the complex geometry into account.

For this test case, we have two kinds of cells, associated respectively with the nonsymmetric and the sinusoidal roughness. For the nonsymmetric roughness, the cell is the same as in 5.2. For the sinusoidal roughness, the horizontal size of the cell is 1.6, and the cell is artificially truncated at $y_2 = 5$. The amplitude of the roughness in the microscopic coordinates is 0.8.

The computed constants for the symmetric roughness are

$$\overline{\chi^1} = -0.3, \quad \overline{\chi^2} = 9\ 10^{-5}, \quad \overline{\chi^3} = -0.05.$$

For the first- and second-order effective boundary value problems, the wall law is imposed on the line $x_2 = \delta = 0.025$. The number of elements used for the boundary value problems on the flat wall is around 2400, i.e. five times less than for the direct computation.

On Fig. 8 the contour lines of respectively χ_1^1, χ_1^2, and χ_1^3 for the sinusoidal geometry are displayed, as well as a plot of their value on the cross section $y_1 = 0.8$. The convergence to a constant vector appears clearly.

On Fig. 9 and Fig. 10, we show the contour lines for the horizontal component of the velocity and the pressure for the direct computation and the three approximations. Here again, the zeroth order condition is not accurate enough, while the other two lead to visible improvements. On Fig. 11, we present the horizontal velocity on the cross sections $x_2 = 0.025$ (just above the rough wall) and $x_2 = 0.035$. Note that the oscillations caused by the rough wall are smoothed when x_2 grows from 0.025 to 0.035. It can be seen that the second-order effective boundary condition led to a better approximation of the solution than the first order. This is best seen on a zoom (see Fig. 12).

The friction coefficient at $x_2 = 0.045$ is plotted on Fig. 13. Here also, the second-order effective boundary condition permits us to approximate the solution better than the first order does. However, the first-order condition is already very accurate, and it is not sure that it is worth using the second-order condition.

5.4. *A Rough Backward-Facing Step*

We deal now with a backward-facing step case at Reynolds number 250. The geometry is displayed on Fig. 14. Here again, there are two kinds of roughness. For this case, there is a recirculation behind the step.

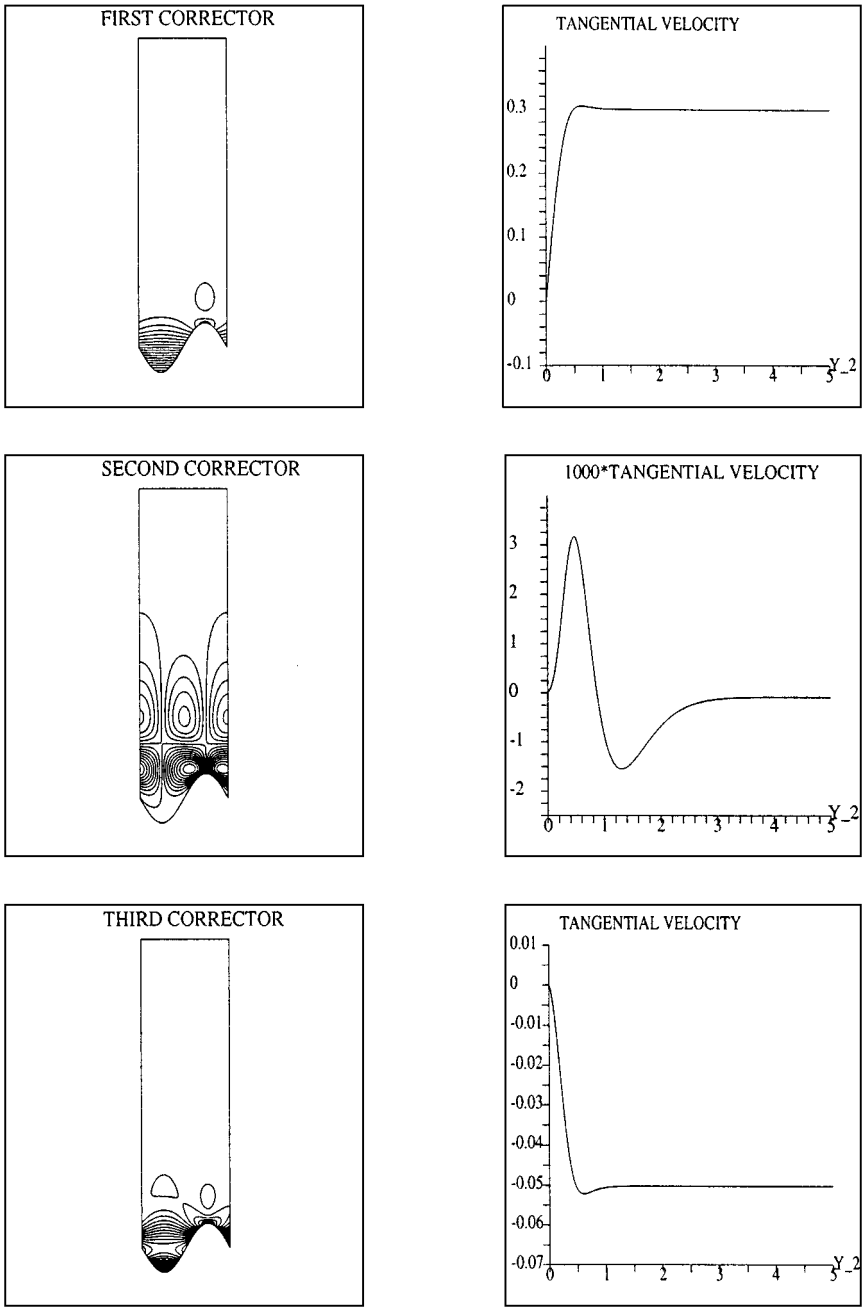

FIG. 8. Contour lines of χ_1^1, χ_1^2, and χ_1^3 for the symmetric roughness and cross sections $y_2 = 0.8$.

On Fig. 15 we plot the tangential velocity and the friction coefficient behind the step at 0.55 above the wall. Here, it is very clear that the second-order wall law performs much better than the first-order one, especially in the recirculation, and the approximation is very good. Only the second-order wall catches the size of the recirculation.

Finally, the streamlines are displayed on Fig. 16.

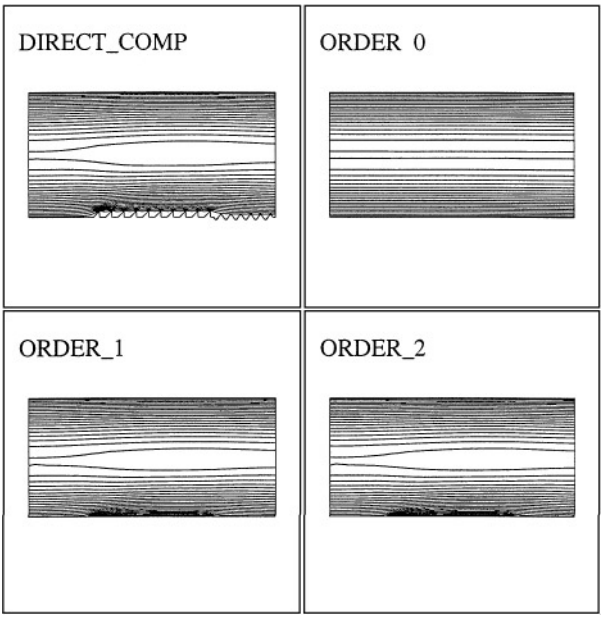

FIG. 9. The horizontal velocity for the four Navier–Stokes problems.

6. APPENDIX

6.1. *Proof of Theorem 3.1*

In order to simplify the notations, we shall drop in the proof the superscripts in χ^1 and π^1. We will write χ for χ^1 and π for π^1.

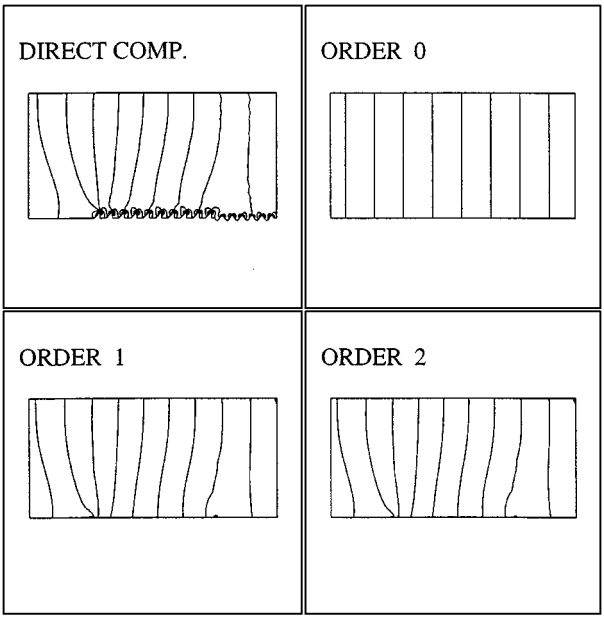

FIG. 10. The pressure for the four Navier–Stokes problems.

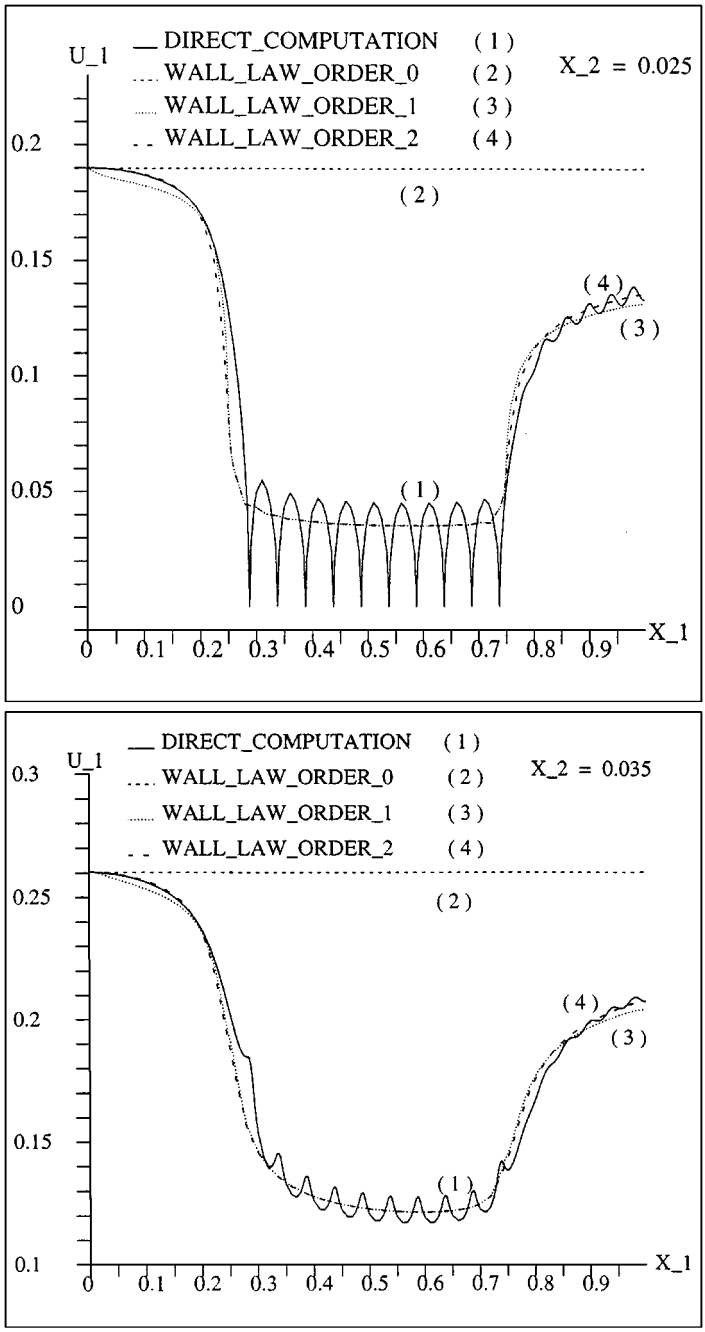

FIG. 11. u_1 on the cross sections $x_2 = 0.025$ and $x_2 = 0.035$.

The proof consists of studying an equivalent boundary value problem in a bounded domain obtained by truncating the cell Y in the y_2 direction. In order to simplify the notations, let us assume that $\mu = 1$. Let $Y_H = Y \cap \{y_2 < H\}$ and Σ_H be the section $\partial Y_H \cap \{y_2 = H\}$. Assume that the cell problem (24) has a solution (χ, π).

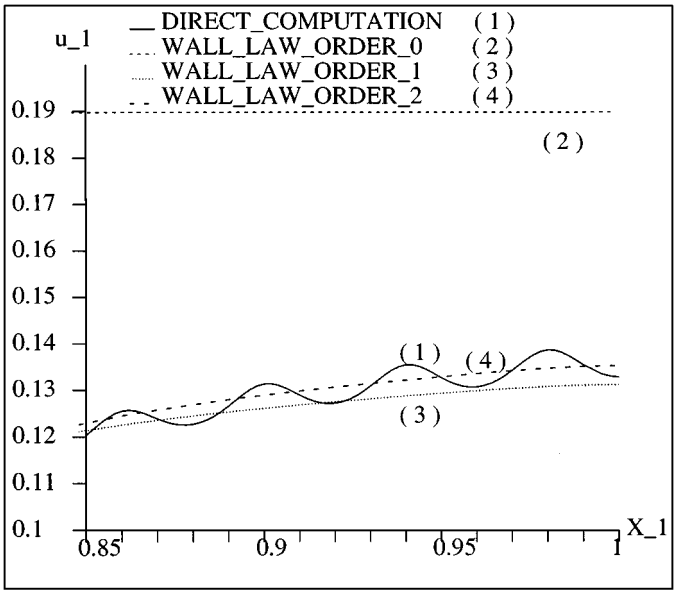

FIG. 12. Zoom of Fig. 11 (up) above the sinusoidal rugosities.

Then, in $y_2 \geq H$, these functions can be expanded in a Fourier series in the variable y_1,

$$\chi_1(y) = \sum_{k=-\infty}^{+\infty} \chi_{1,k}(y_2)\, e^{iky_1},$$

$$\chi_2(y) = \sum_{k=-\infty}^{+\infty} \chi_{2,k}(y_2)\, e^{iky_1},$$

$$\pi(y) = \sum_{k=-\infty}^{+\infty} \pi_k(y_2)\, e^{iky_1},$$

where χ_1, χ_2 are the components of χ, and $\chi_{1,k}$ (resp. $\chi_{2,k}$) is the kth Fourier coefficient of the first (resp. second) component of χ. The Fourier coefficients $\chi_{1,k}$, $\chi_{2,k}$, and π_k are functions of y_2 for $y_2 \geq H$. Since the Stokes equations are homogeneous in the half-space $y_2 > H$, we obtain easily the following set of ordinary differential equations for the kth Fourier coefficients ($k \neq 0$) of χ and π:

$$\begin{aligned} -\chi''_{1,k} + k^2\chi_{1,k} + ik\pi_k &= 0, \\ -\chi''_{2,k} + k^2\chi_{2,k} + \pi'_k &= 0, \\ ik\chi_{1,k} + \chi'_{2,k} &= 0. \end{aligned} \tag{41}$$

The solution of (41) can be computed if $\chi(H)$ is known. Skipping the details we obtain that for $k \neq 0$,

$$\begin{aligned} \chi_{1,k}(y) &= (\chi_{1,k}(H) + k(-\mathrm{sgn}(k)\chi_{1,k}(H) - i\chi_{2,k}(H))(y-H))\, e^{-k(y-H)}, \\ \chi_{2,k}(y) &= (\chi_{2,k}(H) + k(-i\chi_{1,k}(H) + \mathrm{sgn}(k)\chi_{2,k}(H))(y-H))\, e^{-k(y-H)}, \\ \pi_k(y) &= 2k(\mathrm{sgn}(k)\chi_{2,k}(H) - i\chi_{1,k}(H))\, e^{-k(y-H)}, \end{aligned} \tag{42}$$

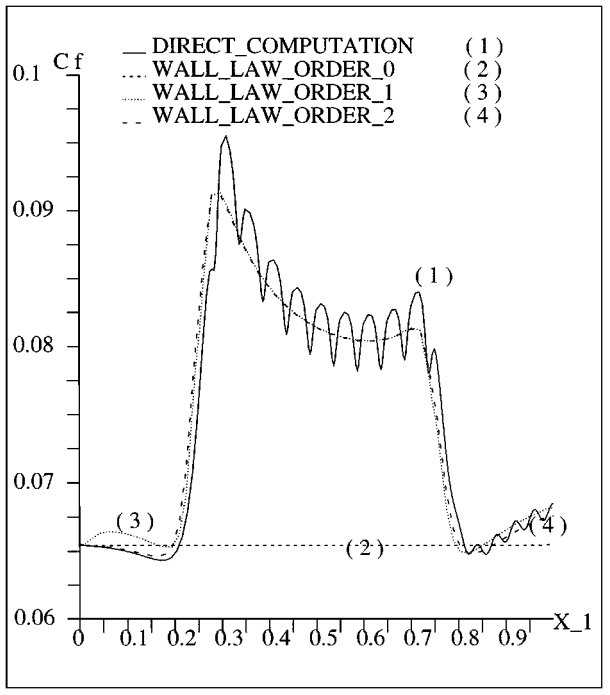

FIG. 13. $C_f = \mu\varepsilon(\partial u_1/\partial x_2)$ on the cross section $x_2 = 0.045$.

where sgn(k) is the sign of k. It is also easy to obtain that $\chi_{1,0}$ and $\chi_{2,0}$ do not depend on y_2. We define $\langle\chi\rangle$ by

$$\langle\chi\rangle = (\chi_{1,0}, \chi_{2,0}).$$

The pressure π is defined up to a constant. From (42), it is possible to find the derivatives

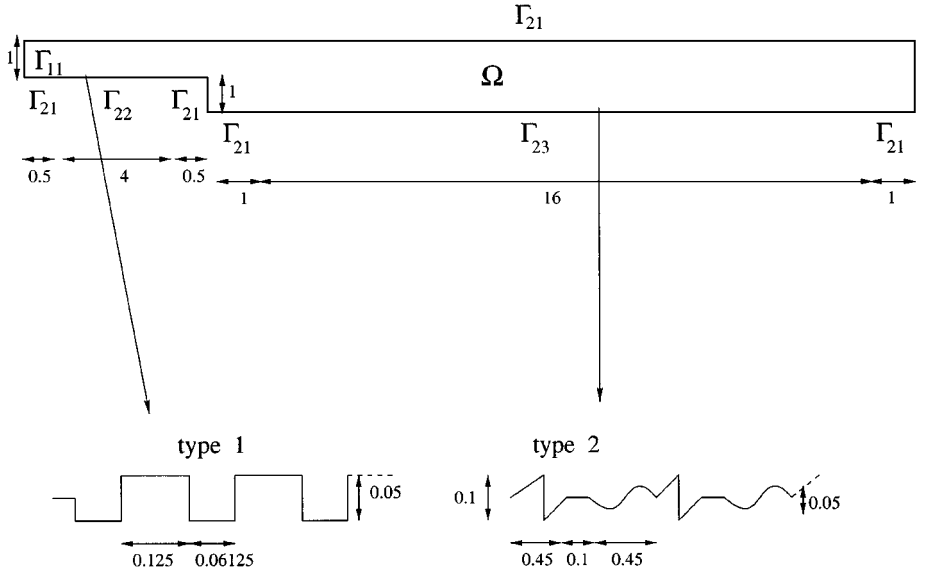

FIG. 14. A rough backward facing step.

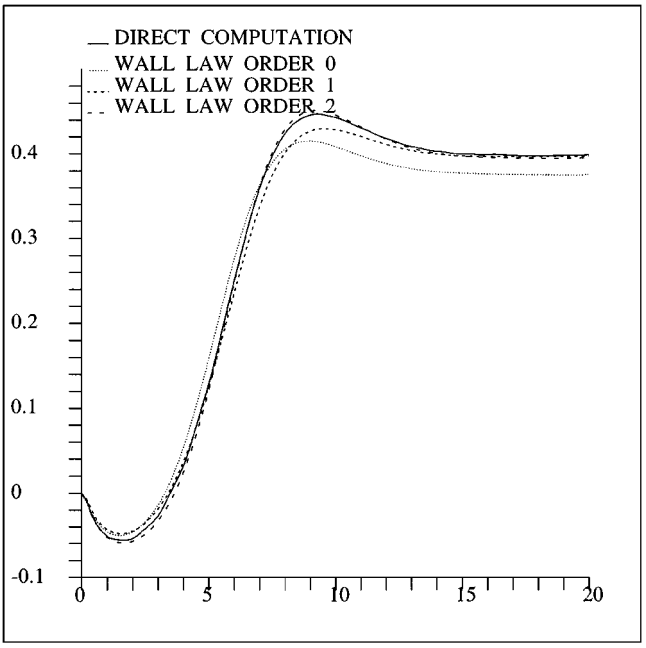

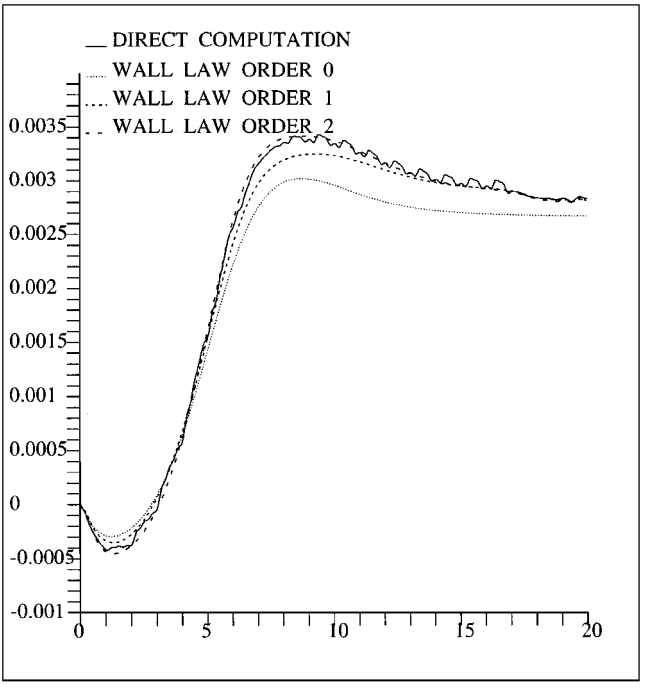

FIG. 15. u_1 (up) and $C_f = \mu\varepsilon(\partial u_1/x_2)$ (bottom) on the cross section $x_2 = 0.55$ above the wall, behind the step.

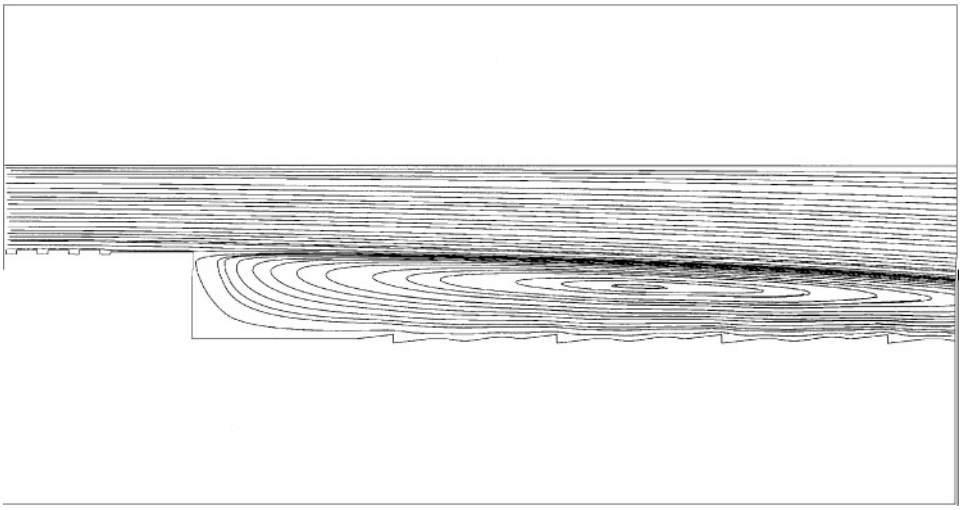

FIG. 16. Direct computation: streamlines behind the step.

of the Fourier coefficients at $y_2 = H$:

$$\begin{aligned} \frac{\partial}{\partial y_2}\chi_{1,k}(H) &= k(-2\chi_{1,k}(H) - i\,\mathrm{sgn}(k)\chi_{2,k}(H)) \\ \frac{\partial}{\partial y_2}\chi_{2,k}(H) - \pi_k(H) &= k(-2\chi_{2,k}(H) - i\,\mathrm{sgn}(k)\chi_{1,k}(H)). \end{aligned} \tag{43}$$

Therefore, on Σ_H we have the transparent boundary condition,

$$-\frac{\partial}{\partial y_2}\chi + \pi e_2 = T\chi, \quad \text{on } \Sigma_H, \tag{44}$$

where T is the integro-differential operator defined by

$$T\chi = \begin{pmatrix} \sum_{k=-\infty}^{+\infty} k(2\chi_{1,k}(H) + i\,\mathrm{sgn}(k)\chi_{2,k}(H))\, e^{iky_1} \\ \sum_{k=-\infty}^{+\infty} k(2\chi_{2,k}(H) - i\,\mathrm{sgn}(k)\chi_{1,k}(H))\, e^{iky_1} \end{pmatrix}. \tag{45}$$

It can be proved that the boundary value problem is equivalent to finding χ and π such that

$$\begin{aligned} -\Delta_y\chi + \nabla_y\pi &= 0, && \text{in } Y_H, \\ \nabla_y \cdot \chi &= 0, && \text{in } Y_H, \\ \chi &= -y_2\, e_1, && \text{on } \partial Y_3 \cup \partial Y_4, \\ -\frac{\partial}{\partial y_2}\chi + \pi e_2 &= T\chi, && \text{on } \Sigma_H, \end{aligned} \tag{46}$$

and then extend χ and π to the whole cell Y by Eqs. (42). For the weak formulation of (46), we introduce the space $H^1_{\mathrm{per}}(Y_\delta)$. Let us prove existence and uniqueness for the variational

formulation of (46). We are going to look for χ in the space $\mathcal{H}$,

$$\mathcal{H} = \left\{ \chi \in \left(H^1_{\text{per}}(Y_H) \right)^2, \nabla_y \cdot \chi = 0 \text{ in } Y_H \right\},$$

and we denote by $\mathcal{H}_0$ the space

$$\mathcal{H}_0 = \{ \chi \in \mathcal{H}, \chi = 0 \text{ on } \partial Y_3 \cup \partial Y_4 \}.$$

The weak formulation of (46) consists of finding $\tilde{\chi} = \chi + y_2 e_1$ satisfying $\tilde{\chi} \in \mathcal{H}_0$ and

$$\forall \eta \in \mathcal{H}_0, \quad \int_{Y_H} \nabla \tilde{\chi} \cdot \nabla \overline{\eta} + \langle T \tilde{\chi}, \overline{\eta} \rangle = \int_{\Sigma_H} e_1 \cdot \overline{\eta}, \tag{47}$$

where $\overline{\eta}$ is the complex conjugate of η. The sesquilinear form

$$(\xi, \eta) \mapsto \int_{Y_H} \nabla \xi \cdot \nabla \overline{\eta} + \langle T \xi, \overline{\eta} \rangle$$

is continuous and hermitian positive definite and, thus, coercive in $\mathcal{H}_0$. Therefore, problem (46) has a unique solution, and the imaginary parts of the solution are clearly 0.

Let us now prove that $\langle \chi \rangle$ is a horizontal vector; indeed,

$$\begin{aligned}
&\int_{Y_\delta} \nabla_y \cdot \chi = 0 \\
&\quad \Rightarrow \quad \int_{y_2=\delta} \chi_2 + \int_{\partial Y_3} \chi \cdot n + \int_{\partial Y_4} \chi \cdot n = 0 \\
&\quad \Rightarrow \quad \int_{y_2=\delta} \chi_2 - \int_{\partial Y_3} y_2 \, e_1 \cdot n - \int_{\partial Y_4} y_2 \, e_1 \cdot n = 0 \\
&\quad \Rightarrow \quad \int_{y_2=\delta} \chi_2 - \int_{Y_\delta} \nabla_y \cdot (y_2 \, e_1) = 0 \\
&\quad \Rightarrow \quad \int_{y_2=\delta} \chi_2 = 0.
\end{aligned}$$

Letting δ go to infinity, we obtain the desired result.

6.2. *Proof of Theorem 3.2*

Let H be greater than $H_{\max}$. From the proof of Theorem 3.1, we obtain that

$$2\pi(\overline{\chi^1} + H) = \int_{Y_H} \nabla\left(\chi^1 + y_2 \, e_1\right) \cdot \nabla\left(\chi^1 + y_2 \, e_1\right) + \langle T \chi^1, \chi^1 \rangle \geq 0,$$

from the positivity of T. The upper bound on $-\overline{\chi^1}$ is obtained by letting H go to $H_{\max}$.

For the lower bound on $-\overline{\chi^1}$, we first notice that the variational formulation for $\chi^1 + y_2 e_1$ is the Euler equation for the minimization problem,

$$\inf_{\xi \in \mathcal{H}_0} \frac{1}{2} \left(\int_{Y_H} \nabla \xi \cdot \nabla \overline{\xi} + \langle T \xi, \overline{\xi} \rangle \right) - \text{Re} \left(\int_{\Sigma_H} e_1 \cdot \xi \right),$$

and that $\overline{\chi^1}$ can be found by

$$-\pi(\overline{\chi^1}+H)=\inf_{\xi\in\mathcal{H}_0}\frac{1}{2}\left(\int_{Y_H}\nabla\xi\cdot\nabla\bar{\xi}+\langle T\xi,\bar{\xi}\rangle\right)-\mathrm{Re}\left(\int_{\Sigma_H}e_1\cdot\xi\right).$$

Let $\widetilde{Y_H}$ be the rectangular domain $\widetilde{Y_H}=(0,2\pi)\times(0,H)$ and let $\tilde{\mathcal{H}}_0$ be the space $\tilde{H}_0=\{\xi\in H^1_{\mathrm{per}}(\widetilde{Y_H});\ \mathrm{div}\,\xi=0;\ \xi(y_1,0)=0\}$. Clearly, $\mathcal{H}_0$ can be viewed as a subspace of $\tilde{\mathcal{H}}_0$ (by extending the functions by 0). Therefore,

$$-\pi(\overline{\chi^1}+H)\geq\inf_{\xi\in\tilde{\mathcal{H}}_0}\frac{1}{2}\left(\int_{Y_H}\nabla\xi\cdot\nabla\bar{\xi}+\langle T\xi,\bar{\xi}\rangle\right)-\mathrm{Re}\left(\int_{\Sigma_H}e_1\cdot\xi\right).$$

This infimum is clearly obtained by the function y_2e_1 and is equal to $-\pi H$. The lower bound on $-\overline{\chi^1}$ follows.

REFERENCES

1. Y. Achdou, Effet d'un mince revêtement métallisé sur la réflexion d'une onde électromagnétique, *C.R. Acad. Sci. Paris Sér. I* **314**, 217 (1992).
2. Y. Achdou and O. Pironneau, Analysis of wall laws, *C.R. Acad. Sci. Paris Sér. I* **320**, 541 (1995).
3. Y. Achdou, P. Letallec, O. Pironneau, and F. Valentin, Constructing wall laws with domain decomposition or asymptotics expansion techniques, *Comput. Methods Appl. Mech. Eng.* **151**, 215 (1997).
4. M. Artola and M. Cessenat, Diffraction d'une onde électromagnétique par une couche composite mince accolée à un conducteur épais, *C.R. Acad. Sci. Paris Sér. I* **313**, 231 (1991).
5. A. Benssousan, J. L. Lions, and G. Papanicolaou, *Asymptotic Analysis for Periodic Structures* (North Holland, Amsterdam, 1983).
6. A. Carrau, *Modélisation Numérique d' un écoulement sur paroi rugueuse*, Ph.D. thesis, Université de Bordeaux, 1992.
7. A. Carrau, G. Gallice, and P. Letallec, Taking into account surface roughness in computing hypersonic reentry bodies, in *Applied Sciences and Engineering*, edited by R. Glowinski (Elsevier, Amsterdam, 1992), p. 331.
8. G. Dury and Alziary de Roquefort, Couche limite turbulente sur paroi rugueuse en regime supersonique, Technical report, CEAT, 1995.
9. R. Fournier, *Vigie User Guide* (INRIA, Sophia-Antipolis, 1997).
10. L. P. Franca and S. L. Frey, Stabilized finite element methods. II. The incompressible Navier–Stokes equations, *Comput. Methods Appl. Mech. Engrg.* **99**(2–3), 209 (1992).
11. F. Glikson, *Couche limite sur paroi rugueuse*, Ph.D. thesis, Ecole Supérieure d'Aéronautique, Toulouse, ONERA CERT Poitiers, 1996.
12. T. J. R. Hughes, *The Finite Element Method* (Prentice–Hall, Englewood Cliffs, NJ, 1987).
13. J. B. Keller, Removing small features from computational domains, *J. Comput. Phys.* **113**, 148 (1994).
14. L. Landau and F. Lifschitz, *Fluid Mechanics* (MIR, Moscow, 1953).
15. J. Nikuradse, Law of flow in rough pipe, Technical report, National advisory commitee for aeronautics, 1929.
16. Y. Saad, *Numerical Methods for Large Eigenvalue Problems* (Manchester Univ. Press, Manchester, 1992).
17. E. Sanchez-Palencia, *Nonhomogeneous Media and Vibration Theory*, Lecture Notes in Physics (Springer-Verlag, Berlin, 1987).
18. F. Valentin, Ph.D. thesis, Université Paris 6, 1998.
19. F. Valentin, Méthode d'élement finis stabilisée pour les équations de Navier–Stokes incompressibles avec des conditions aux limites équivalentes, Technical report, INRIA, to appear.